

Title: Optimization and characterization of a carbamate inhibitor for plasma platelet-activating factor acetylhydrolase (pPAFAH)

Authors: Joseph M G Nagano*, Ku-Lung Hsu*, Anna E Speers*, Steven J Brown*, Timothy Spicer[†], Virneliz Fernandez-Vega[†], Jill Ferguson*, Brian J Bahnson[‡], Benjamin F Cravatt*, Peter Hodder[†], and Hugh Rosen*

*The Scripps Research Institute, La Jolla CA; [†]The Scripps Research Institute, Jupiter, FL; [‡]University of Delaware, Newark, DE.
Corresponding author: hrosen@scripps.edu

Assigned Assay Grant #: 1 R01 HL084366

Screening Center Name & PI: The Scripps Research Institute Molecular Screening Center (SRIMSC), H Rosen

Chemistry Center Name & PI: SRIMSC, H Rosen

Assay Submitter & Institution: BJ Bahnson, Univ. of DE; BF Cravatt, TSRI, La Jolla

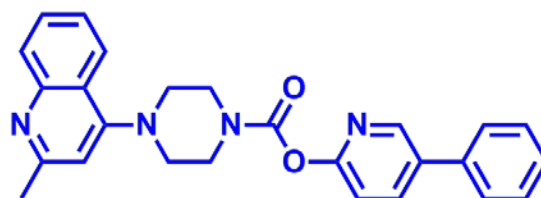
PubChem Summary Bioassay Identifier (AID): 463092

Abstract: Oxidative stress has been implicated as an underlying inflammatory factor in several disease pathologies, including cancer, atherosclerosis, aging, and various neurodegenerative disorders. Phospholipids in particular are susceptible to oxidative damage, and it is thought that the plasma platelet-activating factor acetylhydrolase (pPAFAH, a.k.a. PLA2G7) may facilitate turnover of oxidized phospholipids via hydrolysis of their oxidatively truncated acyl chains. However, there are no commercially available, selective, and *in vivo*-active inhibitors for investigation of pPAFAH biology. As such, we initiated a fluorescence polarization activity-based protein profiling (fluopol-ABPP) high throughput screening (HTS) campaign to identify potential inhibitors of pPAFAH and three PFAFH family members: PFAFH2, PFAFHb2, and PFAFH1b3.

The pPAFAH HTS campaign revealed a large number (~5000) of potential lead compounds, but secondary gel-based screening of ~150 cherry picked top inhibitors quickly revealed the carbamate as a promising scaffold for inhibitor design. Given that carbamate inhibitors for serine hydrolase enzymes have previously been found to have tunable potency and selectivity and good activity *in vivo*, we endeavored to derive a pPAFAH-selective probe from the carbamate scaffold. In this effort, we were aided by the recent identification of a lead pPAFAH carbamate inhibitor from a small in-house library. By combining elements of both the HTS carbamate hits and our in-house lead, the medchem optimized probe (ML256, SID 125269079) is highly potent against its target enzyme (IC₅₀ = 31 nM mouse isoform; 6 nM human isoform), and is active *in situ* and *in vivo*, showing excellent oral bioavailability and blood-brain barrier penetration. ML256 is at least 322-fold selective for all other brain serine hydrolases (~20) assessed by gel-based competitive activity-based protein profiling (ABPP), and is selective for other PFAFH enzymes as determined by both gel-based screening and multidimensional LC-MS/MS analysis (ABPP-

MudPIT). ML256 inhibits pPAFAH by irreversible carbamoylation of the active site serine. The complete properties, characterization, and synthesis of ML256 are detailed in this report.

Probe Structure & Characteristics:



ML256

CID/ML#	Target Name	Target IC50 (nM) [SID, AID]	Anti-target Name(s)	Anti-target IC50 (nM) [SID, AID]	Fold Selective [†]	Secondary Assay(s) Name: IC50 (nM) [SID, AID]
CID 53364507/ ML256	pPAFAH (Pla2g7)	Mouse: 31 [SID 125269079, AID 588770]	>20 brain SHs*	>10,000 [SID 125269079, AID 588774]**	>322	Inhibition Assay: [SID 125269079, AID 588774] Selectivity Assay: [SID 125269079, AID 588774, AID 588767] MudPIT Selectivity Assay: [SID 125269079, AID 588785 and AID 588787] In Situ Assay: [SID 125269079, AID 588817] In Vivo Assay: [SID 125269079, AID 588823] IC50 Assay: mouse 31 nM [SID 125269079, AID 588770]; human 6 nM [SID 125269079, AID 588766] Cytox assay: [SID 125269079, AID 588768] LC-MS/MS assay: [SID 125269079, AID 588788]
		Human: 6 [SID 125269079, AID 588766]	PAFAH2 (closest homolog)	>10,000 [SID 125269079, AID 588767]**	>322	

*As assessed by gel-based competitive ABPP in the mouse brain membrane proteome with the serine hydrolase-specific activity-based probe FP-Rhodamine

**IC50 of the anti-target is defined as greater than the test compound concentration at which less than or equal to 50% inhibition of the anti-target is observed, which is reported in AID 588774. For SID 125269079, no anti-targets were observed for all serine hydrolases (SHs) assayed at 10,000 nM concentration, so the IC50 is reported as >10,000 nM.

[†]Fold-selectivity was calculated as: >IC50 for anti-target/IC50 for pPAFAH

Recommendations for scientific use of the probe:

Oxidative stress has been implicated as an underlying inflammatory factor in numerous disease pathologies, including cancer, atherosclerosis, aging, and neurodegenerative disorders [1-5]. Phospholipids in particular are susceptible to oxidative damage, and it is thought that pPAFAH may facilitate turnover of oxidized phospholipids via hydrolysis of their oxidatively truncated acyl chains. ML256, described herein, is a potent and specific inhibitor of pPAFAH *in vitro*, *in situ*, and *in vivo*. As such, it is recommended for use in primary research studies aimed at elucidating the patho/physiological roles and substrate specificity of pPAFAH and its contribution to inflammatory disease processes.

1 Introduction

Oxidative stress has been implicated as an underlying inflammatory factor in several disease pathologies, including cancer, atherosclerosis, aging, and various neurodegenerative disorders [1-5]. Phospholipids in particular are susceptible to oxidative damage, and (per)oxidized phospholipids can have deleterious effects, including disruption of membrane bilayers and production of toxic byproducts [4, 6-8]. One hypothesized pathway for removal of oxidatively damaged lipids involves hydrolysis by phospholipase A2-type enzymes. Candidate hydrolytic enzymes include the platelet-activating factor acetylhydrolases (PAFAHs) [4, 9]. The initial role assigned to the PAFAHs was the hydrolysis of platelet activating factor (PAF) [10, 11], a potent pro-inflammatory phospholipid signaling molecule [12], which plays a role in myriad physiological processes including inflammation, anaphylaxis, fetal development, and reproduction [4, 13]. The PAFAHs are subdivided into three classes: plasma (p)PAFAH (a.k.a. PLA2G7), and intracellular types 1 and 2. In terms of sequence homology, pPAFAH and PAFAH2 are close homologs and show little similarity to type 1 enzymes.

A large number of studies have been published over the years since pPAFAH was first discovered linking an increase in pPAFAH concentration and/or activity to an increased risk of various cardiovascular diseases [14, 15]. The biological function of pPAFAH in the development of coronary heart diseases (CHD) is controversial, with both anti- and proinflammatory roles attributed to it [16, 17]. Chemical tools capable of interrogating enzyme architecture (co-crystallization studies) and providing precise temporal control over activity of pPAFAH and the other PAFAH-family enzymes are necessary for complete characterization of substrate specificity and patho/physiological roles of the PAFAHs in phospholipid metabolism and inflammatory disease processes. Towards that goal, we developed a HTS assay for inhibitor discovery for four PAFAH enzymes: pPAFAH, PAFAH2, PAFAH1b2, and PAFAH1b3, based on their reactivity with the serine-hydrolase-specific fluorophosphonate (FP) [18] activity-based protein profiling (ABPP) probe. This reactivity can be exploited for inhibitor discovery using a competitive-ABPP platform, whereby small molecule enzyme inhibition is assessed by the ability to out-compete ABPP probe labeling [19]. Competitive ABPP has also been configured to operate in a high-throughput manner via fluorescence polarization readout, fluopol-ABPP [20]. This HTS campaign followed by medchem optimization has already delivered an optimized triazole urea probe for PAFAH2, ML225. Following the fluopol-ABPP HTS campaign for pPAFAH and secondary gel-based competitive ABPP screening, we identified several carbamate hit compounds with IC50s of 200-400 μ M. By combining structural elements of these compounds with an in-house carbamate lead, **WWL153** (SID 99205832), we derived probe ML256 (SID 125269079), which is highly potent against pPAFAH (IC50 31 nM for the mouse isoform, 6 nM for the human isoform), and is active *in situ* and *in vivo*, inhibiting its target enzyme in the mouse brain following oral administration. ML256 is at least 322-fold selective for

all other brain serine hydrolases (SHs) (~20) assessed by gel-based competitive ABPP, and is selective for the counter-screen enzymes pPAFAH, PAFAH1b2, and PAFAH1b3. ML256 inhibits its target by carbamoylating the active site serine. While reversible inhibitors (darapladib) of pPAFAH have been reported [21], these compounds are not commercially available and have not been extensively characterized *in vivo* due to the lack of known biomarkers to assess pPAFAH inhibition in living systems. ML256 is the first selective, covalent inhibitor of pPAFAH, and we show that its activity against pPAFAH can be evaluated in living systems, including mice, using competitive ABPP methods.

2 Materials and Methods

All reagents for chemical synthesis were obtained from ThermoFisher or SigmaAldrich. All other protocols are summarized in **Section 2.1**.

2.1 Assays

Probe Characterization Assays

Solubility

The solubility of compounds was tested in phosphate buffered saline, pH 7.4. Compounds were inverted for 24 hours in test tubes containing 1-2 mg of compound with 1 mL of PBS. The samples were centrifuged and analyzed by HPLC (Agilent 1100 with diode-array detector). Peak area was compared to a standard of known concentration.

Stability

Demonstration of stability in PBS was conducted under conditions likely to be experienced in a laboratory setting. The compound was dissolved in 1 mL of PBS at a concentration of 10 μ M, unless its maximum solubility was insufficient to achieve this concentration. Low solubility compounds were tested between ten and fifty percent of their solubility limit. The solution was immediately aliquoted into seven standard polypropylene microcentrifuge tubes which were stored at ambient temperature in a block microcentrifuge tube holder. Individual tubes were frozen at -80°C at 0, 1, 2, 4, 8, 24, and 48 hours. The frozen samples were thawed in a room temperature and an equal volume of acetonitrile was added prior to determination of concentration by LC-MS/MS.

LC-MS/MS for stability assay

All analytical methods are in MRM mode where the parent ion is selected in Q1 of the mass spectrometer. The parent ion is fragmented and a characteristic fragment ion is monitored in Q3. MRM mass spectroscopy methods are particularly sensitive because additional time is spent monitoring the desired ions and not sweeping a large mass range. Methods will be rapidly set up using Automaton[®] (Applied Biosystems), where the compounds are listed with their name

and mass in an Excel datasheet. Compounds are submitted in a 96-well plate to the HPLC autosampler and are slowly injected without a column present. A narrow range centered on the indicated mass is scanned to detect the parent ion. The software then evaluates a few pre-selected parameters to determine conditions that maximize the signal for the parent ion. The molecule is then fragmented in the collision cell of the mass spectrometer and fragments with m/z larger than 70 but smaller than the parent mass are determined. Three separate collision energies are evaluated to fragment the parent ion and the largest three ions are selected. Each of these three fragment ions is further optimized and the best fragment is chosen. The software then inserts the optimized masses and parameters into a template method and saves it with a unique name that indicates the individual compound being optimized. Spectra for the parent ion and the fragmentation pattern are saved and can be reviewed later.

Determination of glutathione reactivity

One μL of a 10 mM compound stock solution was added to 1 mL of a freshly prepared solution of 100 μM reduced glutathione. Final compound concentration is 10 μM unless limited by solubility. The solution was allowed to incubate at 37°C for two hours prior to being directly analyzed for glutathione adduct formation. LC-MS/MS analysis of GSH adducts was performed on an API 4000 Q-Trap™ mass spectrometer equipped with a Turboionspray source (Applied Biosystems, Foster City, CA). Two methodologies were utilized: a negative precursor ion (PI) scan of m/z 272, corresponding to GSH fragmenting at the thioether bond, and a neutral loss scan of -129 AMU to detect GSH adducts. This triggered positive ion enhanced resolution and enhanced product ion scans [22, 23].

Primary Assays

Primary uHTS assay to identify pPAFAH inhibitors (AID 463082)

Assay Overview: The purpose of this assay is to identify compounds that act as inhibitors of the plasma platelet activating factor acetylhydrolase (pPAFAH). In this biochemical assay, recombinant human pPAFAH protein (purified GST-fusion construct expressed in *E. coli* BL21 cells, contains residues 42-441 plus a non-native N-terminal extension [GSPNSRVD] and three mutations in the hydrophobic patch region: I120A, L123A, L124A) is incubated with test compounds for a defined period, followed by addition of a rhodamine-conjugated fluorophosphonate (FP-Rh) serine hydrolase-specific activity-based probe. The reaction is excited with linear polarized light and the intensity of the emitted light is measured as the polarization value. As designed, test compounds that act as pPAFAH inhibitors will prevent pPAFAH-probe interactions, thereby increasing the proportion of free (unbound) fluorescent probe in the well, leading to low fluorescence polarization. Compounds are tested in singlicate at a final nominal concentration of 3.39 μM

Protocol Summary: Prior to the start of the assay, 4.0 μL of Assay Buffer (0.01% pluronic detergent, 50 mM Tris HCl pH 8.0, 150 mM NaCl, 1 mM DTT) containing 12.5 nM pPAFAH protein were dispensed into 1536 microtiter plates. Next, 17 nL of test compound in DMSO or DMSO alone (0.34% final concentration) were added to the appropriate wells and incubated for 30 minutes at 25°C. The assay was started by dispensing 1.0 μL of 375 nM FP-Rh probe in

Assay Buffer to all wells. Plates were centrifuged and incubated for 15 minutes at 25°C, and fluorescence polarization was read on a Viewlux microplate reader (PerkinElmer, Turku, Finland) using a BODIPY TMR FP filter set and a BODIPY dichroic mirror (excitation = 525 nm, emission = 598 nm) for 15 seconds for each polarization plane (parallel and perpendicular). **Assay Cutoff:** Compounds that inhibited pPAFAH $\geq 24.55\%$ were considered active.

Confirmation uHTS assay to identify pPAFAH inhibitors (AID 463230)

Assay Overview: The purpose of this assay is to confirm activity of compounds identified as active in the primary uHTS pPAFAH screen (AID 463082). In this assay, the FP-Rh probe was used to label pPAFAH in the presence of test compounds and analyzed as described previously (AID 463082). Compounds were tested in triplicate at a nominal concentration of 3.39 μM .

Protocol Summary: The assay was performed as described previously (AID 463082), except that compounds were tested in triplicate. **Assay Cutoff:** Compounds that inhibited pPAFAH $\geq 24.55\%$ were considered active.

Secondary Assays

Inhibition of cherry-picked uHTS hits (AID 588474)

Assay Overview: The purpose of this assay is to determine whether test compounds identified as active in the uHTS campaign (AIDs 463082 and 463230) can inhibit over-expressed pPAFAH in a complex proteomic lysate. In this assay, proteome containing pPAFAH is incubated with test compound followed by reaction with an SH-specific FP-Rh activity-based probe. The reaction products are separated by SDS-PAGE and visualized in-gel using a flatbed fluorescence scanner. The percentage activity remaining is determined by measuring the integrated optical density (IOD) of the bands. As designed, test compounds that act as pPAFAH inhibitors will prevent enzyme-probe interactions, thereby decreasing the proportion of bound fluorescent probe, giving lower fluorescence intensity in the band in the gel.

Protocol Summary: Recombinant mouse pPAFAH (25 μL of 0.25 mg/mL membrane proteome preparation from transiently transfected 293T Hek cells overexpressing pPAFAH, Open Biosystems Accession BC010726, in Dulbecco's PBS [DPBS]) was treated with test compound (1 μL of a 25x stock in DMSO, 5 μM final concentration) or DMSO (1 μL) for 30 minutes at 37°C. FP-Rh (1 μL of 25x stock in DMSO; 2 μM final concentration) was added and the reaction was incubated for 30 minutes at 25°C, quenched with 2x SDS-PAGE loading buffer, separated by SDS-PAGE and visualized by in-gel fluorescent scanning. The percentage activity remaining was determined by measuring the IOD of pPAFAH bands relative to a DMSO-only (no compound) control. **Assay Cutoff:** Compounds with $\geq 75\%$ inhibition were considered active.

Inhibition and selectivity of carbamate library members (AIDs 588773 and 588774)

Assay Overview: The purpose of this assay is to determine whether test compounds (either cherry picked uHTS hits [AID 588773] or synthetic medchem compounds [AID 588774]) can

inhibit over-expressed pPAFAH in a complex proteomic lysate and to estimate compound selectivity in an ABPP assay. Test compound is incubated with recombinantly-expressed target enzyme pPAFAH (Assay 1) or serine hydrolase (potential anti-target) rich complex proteome (Assay 2) followed by reaction with an SH-specific FP-Rh activity-based probe. The reaction products are separated by SDS-PAGE and analyzed as described for AID 588474.

Protocol Summary:

Assay 1: Recombinant mouse pPAFAH (50 μ L of 0.25 mg/mL membrane proteome preparation from transiently transfected 293T Hek cells overexpressing pPAFAH, Open Biosystems Accession BC010726) in DPBS was treated with test compound (10, 1, or 0.1 μ M final concentration, 1 μ L of a 50x stock in DMSO) or DMSO (1 μ L) for 30 minutes at 37°C. FP-Rh (1 μ L of a 50 μ M solution in DMSO; 1 μ M final concentration) was added, and the reaction was incubated for 30 minutes at 37°C, quenched with an equal volume of 2x SDS-PAGE loading buffer (reducing), separated by SDS-PAGE, and visualized by in-gel fluorescent scanning. The percentage activity remaining was determined by measuring the integrated optical density of the pPAFAH band relative to a DMSO-only (no compound) control. **Assay Cutoff:** Compounds with \geq 50% inhibition at 0.1 μ M were considered active.

Assay 2: Mouse brain membrane proteome (50 μ L of 1 mg/mL in DPBS) was treated with test compound (10, 1, or 0.1 μ M final concentration, 1 μ L of a 50x stock in DMSO) or DMSO (1 μ L) for 30 minutes at 37°C. FP-Rh (1 μ L of a 25 μ M solution in DMSO; 1 μ M final concentration) was added, and the reactions was incubated for 30 minutes at 37°C, quenched with an equal volume of 2x SDS-PAGE loading buffer (reducing), separated by SDS-PAGE, and visualized by in-gel fluorescent scanning. The percentage activity remaining for each anti-target (fatty acid amide hydrolase [FAAH], monoacylglycerol lipase [MAGL], abhydrolase domain-containing proteins 3, 4, and 6 [ABHD3, ABHD4, ABHD6], lysophospholipases 1 and 2 [LYPLA1, LYPLA2], and unidentified proteins with molecular weight [MW] of 32kDa and 30kDa) was determined by measuring the integrated optical density of the individual protein bands relative to a DMSO-only (no compound) control. **Assay Cutoff:** Compounds with \geq 50% inhibition at 0.1 μ M were considered active.

Selectivity against anti-target PFAH2 (AID 588767)

Assay Overview: The purpose of this assay is to determine whether test compounds can inhibit the pPAFAH anti-target PFAH2 in a gel-based competitive ABPP assay. In this assay, endogenous PFAH2 is incubated with test compound followed by reaction with the SH-specific FP-Rh activity-based probe. The reaction products are separated by SDS-PAGE and analyzed as described for AID 588474.

Protocol Summary: Soluble proteome (1 mg/ml in DPBS) of BW5147-derived murine T cells was treated with test compound (1 μ L of a 50x stock in DMSO; 0.1 μ M, 1 μ M, or 10 μ M final concentration) or DMSO (1 μ L) for 30 minutes at 37 °C. FP-Rh (1 μ L of a 25 μ M solution in DMSO; 1 μ M final concentration) was added, and the reaction was incubated for 30 minutes at 37°C, quenched with an equal volume of 2x SDS-PAGE loading buffer (reducing), separated by SDS-PAGE, and visualized by in-gel fluorescent scanning. The percentage activity remaining

was determined by measuring the IOD of the PAFAH2 band relative to a DMSO-only (no compound) control. **Assay Cutoff:** Compounds with $\geq 50\%$ inhibition at 0.1 μM were considered active.

Determination of IC50 values against mouse pPAFAH (AIDs 588769 and 588770)

Assay Overview: The purpose of this assay is to determine the IC50 values of test compounds (either cherry picked uHTS hits [AID 588769] or synthetic medchem compounds [AID 588770]) for pPAFAH inhibition. In this assay, the SH-specific FP-Rh activity-based probe is used to label pPAFAH in the presence of test compounds. The reaction products are separated by SDS-PAGE and analyzed as described for AID 588474.

Protocol Summary: Recombinant mouse pPAFAH (50 μL of 0.25 mg/mL membrane proteome preparation from transiently transfected 293T Hek cells overexpressing pPAFAH, Open Biosystems Accession BC010726) in DPBS was treated with test compound (1 μL of a 25x stock in DMSO) or DMSO (1 μL) for 30 minutes at 37°C before the addition of FP-Rh (1 μL of 25x stock in DMSO, 1 μM final concentration). The reaction was incubated for 30 minutes at 37°C, quenched with an equal volume of 2x SDS-PAGE loading buffer (reducing), separated by SDS-PAGE and visualized by in-gel fluorescent scanning. The percentage activity remaining was determined by measuring the IOD of the bands relative to a DMSO-only (no compound) control. IC50 values for inhibition of pPAFAH were determined from dose-response curves from three replicates at each inhibitor concentration (7-point 1:3 dilution series from 1 μM to 1 nM).

Assay Cutoff: Compounds with an IC50 ≤ 500 nM were considered active.

Determination of IC50 values against human pPAFAH (AID 588766)

Assay Overview: The purpose of this assay is to determine the IC50 values of test compounds for human pPAFAH inhibition. In this assay, the SH-specific FP-Rh activity-based probe is used to label pPAFAH in the presence of test compounds. The reaction products are separated by SDS-PAGE and analyzed as described for AID 588474.

Protocol Summary: Recombinant, human pPAFAH (25 μL of 1 $\mu\text{g}/\text{mL}$; purified GST-fusion construct expressed in E.coli BL21 cells; protein contains residues 42-441 plus a non-native N-terminal extension (GSPNSRVD), and the following mutations in the hydrophobic patch region: I120A, L123A, L124A) in DPBS was treated with test compound (1 μL of a 25x stock in DMSO) or DMSO (1 μL) for 30 minutes at 37°C before the addition of FP-Rh (1 μL of 25x stock in DMSO, 1 μM final concentration). The reaction was incubated for 30 minutes at 37°C, quenched with an equal volume of 2x SDS-PAGE loading buffer (reducing), separated by SDS-PAGE and visualized by in-gel fluorescent scanning. The percentage activity remaining was determined by measuring the IOD of the bands relative to a DMSO-only (no compound) control. IC50 values for inhibition of pPAFAH were determined from dose-response curves from three replicates at each inhibitor concentration (7-point 1:3 dilution series from 1 μM to 1 nM). **Assay Cutoff:** Compounds with an IC50 ≤ 500 nM were considered active.

Analysis of Cytotoxicity (AID 588768)

Assay Overview: The purpose of this assay is to determine cytotoxicity of inhibitor compounds belonging to the carbamate scaffold. In this assay, 293T Hek cells in either serum-free media (Assay 1) or media containing 10% fetal calf serum (FCS); Assay 2) are incubated with test compounds, followed by determination of cell viability. The assay utilizes the WST-1 substrate which is converted into colorimetric formazan dye by the metabolic activity of viable cells. The amount of formazan generated directly correlates to the number of metabolically active cells in the culture. As designed, compounds that reduce cell viability will result in decreased absorbance of the dye.

Protocol Summary: This assay was started by dispensing 293T Hek cells in DMEM media (100 μ L, 15,000 cells/well) into a 96-well plate. Both serum-free media (Assay 1) and media supplemented with 10% FCS; Assay 2) were tested. Compound (10 μ L of 11x stock solutions in media containing 10% DMSO) was added to each well, cells were incubated for 48 hours at 37°C in a humidified incubator, and cell viability was determined by the WST-1 assay (Roche) according to manufacturer instructions. CC50 values were determined from dose-response curves from five replicates at each compound concentration (7-point 1:5 dilution series starting at a nominal test concentration of 50 μ M). **Assay Cutoff:** Compounds with a CC50 value of \leq 5 μ M were considered active (cytotoxic).

LC-MS/MS Analysis of Inhibitor Binding Mode (AID 588788)

Assay Overview: The purpose of this assay is to assess the covalent nature of an inhibitor compound belonging to the carbamate scaffold and determine whether or not it labels the active site serine of pPAFAH. In this assay, purified enzyme is reacted with inhibitor compound, digested with trypsin, and the resulting peptides are analyzed by liquid chromatography-tandem mass spectrometry (LC-MS/MS). The resulting data are analyzed to identify sites of covalent labeling.

Protocol Summary: Two aliquots of purified, recombinant human pPAFAH (25 μ L of 40 μ M in DPBS; purified GST-fusion construct expressed in *E. coli* BL21 cells; protein contains residues 42-441 plus a non-native N-terminal extension [GSPNSRVD], and the following mutations in the hydrophobic patch region: I120A, L123A, L124A) were prepared. To one aliquot was added test compound (1 μ L of 25x stock in DMSO, 100 μ M final concentration). To the second (control) aliquot was added an equal volume of DMSO. Reactions were gently vortexed and incubated at 37°C for 60 minutes. To each reaction was added freshly prepared urea (75 μ L of 6 M in DPBS), DDT (1.5 μ L of 10 mM), and the reactions were incubated at 65°C for 25 minutes and then allowed to cool to room temperature. To each reaction was then added freshly prepared iodoacetamide (20 μ L of 400 mM), and the reactions were rotated for 30 minutes at 25°C in the dark. Aqueous ammonium bicarbonate (150 μ L of 50 mM) was added, followed by CaCl₂ (1.5 μ L of 100 mM), and sequencing grade modified trypsin (1 μ g). Reactions were incubated at 37°C for 12 hours. The protein digests were acidified with formic acid (5% v/v final).

An Agilent 1200 series quaternary HPLC pump and Thermo Scientific LTQ-Orbitrap mass spectrometer were used for sample analysis. A fraction (20 μ L) of the protein digest for each sample was pressure-loaded onto a 100 micron fused-silica column (with a 5 micron in-house pulled tip) packed with 10 cm of Aqua C18 reversed-phase packing material. Chromatography

was carried out using an increasing gradient of aqueous acetonitrile containing 0.1% formic acid over 125 minutes. Data were collected in data-dependent acquisition mode with dynamic exclusion turned on (60 seconds, repeat of 1). Specifically, one full MS (MS1) scan (400-1800 m/z) was followed by 7 MS2 scans of the most abundant ions. The MS2 spectra data were extracted from the raw file using RAW Xtractor (version 1.9.1; publically available at <http://fields.scripps.edu/downloads.php>). The MS2 spectra generated for each run were searched against the latest version of the IPI human protein database concatenated to a reversed decoy database using Sequest [24]. Search parameters specified a static modification of +57.021 for cysteine due to alkylation, a variable modification of +253.12152 for serine to account for possible compound labeling, and no enzyme specificity. The resulting peptide identifications were assembled into protein identifications using DTASelect (version 2.0.41) using the `-trypstat` and `--modstat` options, which apply different statistical models for the analysis of tryptic, half-tryptic, non-tryptic, and modified peptides. DTASelect 2.0 uses a quadratic discriminant analysis to achieve a user-defined false positive hit rate below 1% (as determined by number of hits against the reversed database) at the peptide level. No modified peptides were identified in the DMSO-treated sample. **Assay Cutoff:** Compounds observed to covalently modify the active site serine of pPAFAH were considered active.

ABPP-MudPIT Analysis of Selectivity (AID 588785 and AID 588787)

Assay Overview: The purpose of this assay is to determine the selectivity profile of test compounds in a complex proteome by ABPP in combination with the multidimensional protein identification technology (MudPIT) [25, 26] LC-MS/MS analysis platform. In this assay, paired complex proteome samples are treated with test compound or DMSO, followed by reaction with the serine hydrolase specific activity-based fluorophosphonate-biotin (FP-biotin) affinity probe. Biotinylated proteins are enriched, trypsinized, and analyzed by MudPIT. Inhibition of target and anti-target activity is quantified by comparing spectra counts between the test compound- and DMSO-treated samples. As designed, compounds that act as inhibitors will block FP-biotin labeling, reducing enrichment in the inhibitor-treated sample relative to the DMSO-treated sample, thus giving a smaller spectra count ratio (test compound/DMSO) for each protein. Proteins not targeted by inhibitors would be expected to have a ratio of 1.

Protocol Summary: Sample Preparation. Paired aliquots of mouse brain soluble proteome (AID 588787) or mouse brain membrane proteome (AID 588785) (1mL of 1 mg/mL in 50 mM Tris pH 8.0 [Tris] buffer) were treated with either 1 μ M test compound (20 μ L of a 50x stock in DMSO) or DMSO for 30 min at 37°C. Each reaction was labeled with 5 μ M of FP-biotin (5 μ L of a 50x stock in DMSO) for 2 hours at 25°C. TritonX100 was added to 1% final concentration (v/v), and the proteomes were desalted over PD-10 desalting columns (GE Healthcare). SDS was added to the eluate to give 0.5% final concentration, and the samples heated to 90°C for 8 minutes. FP-labeled proteins were enriched with streptavidin beads (100 μ L of 50% slurry; 25°C, 1 hour, 8.5 mL total volume Tris). Following enrichment, the beads were washed with 1% SDS in Tris (2x), 6 M Urea in Tris (2x), and Tris (2x), and then resuspended in 8 M urea, reduced with TCEP (10 mM) for 25 minutes at 25°C, and alkylated with iodoacetamide (12.5 mM) for 25 minutes at 25°C in the dark. The urea concentration was reduced to 2 M with Tris, and on-bead digestions were performed for 12 hours at 37°C with sequence-grade modified

trypsin (Promega; 2 µg) in the presence of 2 mM CaCl₂. Peptide samples were acidified to a final concentration of 5% (v/v) formic acid, pressure-loaded on to a biphasic (strong cation exchange/reversed phase) MudPIT capillary column and analyzed as described next. A total of 4 biological replicates were prepared and analyzed for each experiment.

LC-MS/MS analysis. Digested and acidified peptide mixtures were analyzed by two-dimensional liquid chromatography/tandem mass spectrometry (MudPIT) using an Agilent 1200-series quaternary pump and Thermo Scientific LTQ ion trap mass spectrometer. Peptides were eluted in a 5-step MudPIT experiment using 0%, 25%, 50%, 80%, and 100% salt bumps of 500 mM aqueous ammonium acetate, with chromatographic elution following each salt pulse accomplished using an increasing gradient of aqueous acetonitrile containing 0.1% formic acid over 125 minutes. Data were collected in data-dependent acquisition mode with dynamic exclusion turned on (90 s, repeat of 1). Specifically, one full MS (MS1) scan (400-1800 m/z) was followed by 7 MS2 scans of the most abundant ions. The MS2 spectra data were extracted from the raw file using RAW Xtractor (version 1.9.1; publically available at <http://fields.scripps.edu/downloads.php>). MS2 spectra data were searched using the PROLUCID algorithm (publically available at <http://fields.scripps.edu/downloads.php>) against the latest version of the mouse UniProt database concatenated with the reversed database for assessment of false-discovery rates. PROLUCID searches allowed for variable oxidation of methionine (+16), static modification of cysteine (+57 due to alkylation), and no enzyme specificity. The resulting MS2 spectra matches were assembled into protein identifications and filtered using DTASelect (version 2.0.41) using the `-trypstat` and `-modstat` options, which apply different statistical models for the analysis of tryptic, half-tryptic, non-tryptic, and modified peptides. DTASelect 2.0 uses a quadratic discriminant analysis to maintain a user-defined false positive hit rate (as determined by number of hits against the reversed database) below 1% at the peptide level. Spectra count abundance ratios (test compound/DMSO) were calculated for all serine hydrolases with an average of 10 or more spectra counts in the DMSO control samples. **Assay Cutoff:** A compound was considered active for a particular target/anti-target with a spectra count ratio (test compound/DMSO control) of ≤ 0.5 .

Analysis of pPAFAH Inhibition *In Situ* (AID 588817)

Assay Overview: The purpose of this assay is to determine whether or not test compounds can inhibit pPAFAH *in situ*. In this assay, cultured cells are incubated with test compound. Cells are harvested, homogenized, and reacted with the SH-specific FP-Rh activity-based probe. The reaction products are separated by SDS-PAGE and analyzed as described for AID 588474.

Protocol Summary: Transiently transfected 293T Hek cells overexpressing mouse pPAFAH (Open Biosystems Accession BC010726) were cultured in a 6-well dish for 48 hours in DMEM medium containing 10% FCS. Cells were washed with DBPS and fresh, serum-free DMEM medium (1 mL) was added. Cells were treated with test compound (10 µM, 1 µM, 0.1 µM, and 0.01 µM final concentration; 10 µL of 100x stock in DMSO) or DMSO only and incubated for 4 hours at 37°C. Cells were washed with DPBS (4x), harvested, and homogenized by sonication. The soluble and membrane fractions were separated by centrifugation (100K x g, 45 min) and

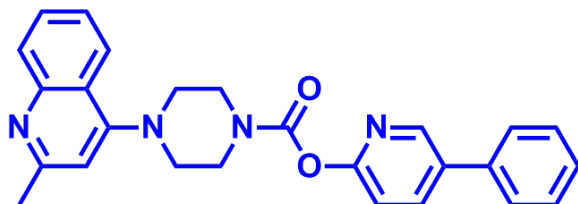
the protein concentration in each fraction was adjusted to 1 mg/mL with DPBS. FP-Rh (1 μ L of 50x stock in DMSO) was added to a final concentration of 1 μ M in 50 μ L total reaction volume. The reaction was incubated for 30 minutes at 37°C, quenched with an equal volume of 2x SDS-PAGE loading buffer, separated by SDS-PAGE and visualized by in-gel fluorescent scanning. The percentage activity remaining was determined by measuring the integrated optical density of the pPAFAH band relative to a DMSO-only (no compound) control. **Assay Cutoff:** Compounds with \geq 50% inhibition at 0.1 μ M compound concentration were considered active.

Analysis of pPAFAH Inhibition *In Vivo* (AID 588789 and AID 588823)

Assay Overview: The purpose of this assay is to determine whether or not test compounds can inhibit pPAFAH *in vivo* (AIDs 588789 and 588823) and to assess selectivity (AID 588823). In this assay, test compounds are orally administered to mice. Mice are sacrificed, and their brain tissue harvested, homogenized, and the membrane fraction isolated and reacted with the activity-based probes HT-01 [27] or FP-Rh. HT-01 bears a BODIPY fluorophore and urea triazole reactive group that selectively labels several serine hydrolases, including pPAFAH. This reagent is used in addition to the standard SH probe FP-Rh to enhance visualization of pPAFAH, which is otherwise obscured by other SHs upon SDS-PAGE separation/visualization. The reaction products are separated by SDS-PAGE and analyzed as described for AID 588474.

Protocol Summary: Purpose-bred WT laboratory mice were orally administered test compound (50 mg/kg in PEG300 vehicle solution) or vehicle only (n = 2 or 4 per group). After four hours, mice were humanely sacrificed (anesthetized with isoflurane and decapitated) and brain tissues removed and snap frozen in liquid nitrogen. Tissues were homogenized and the membrane fraction isolated by centrifugation (45 min, 100K x g) and adjusted to 1 mg/mL in DPBS. Aliquots (50 μ L) were treated with HT-01 (1 μ L of 50x stock in DMSO, 1 μ M final concentration) or FP-Rh (1 μ L of 50x stock in DMSO, 1 μ M final concentration). The reaction was incubated for 30 minutes at 37°C, quenched with an equal volume of 2x SDS-PAGE loading buffer (reducing), separated by SDS-PAGE and visualized by in-gel fluorescent scanning. The percentage activity remaining was determined by measuring the IOD of test compound bands relative to vehicle bands. **Assay Cutoff:** Compounds with \geq 50% inhibition were considered active.

2.2 Probe Chemical Characterization



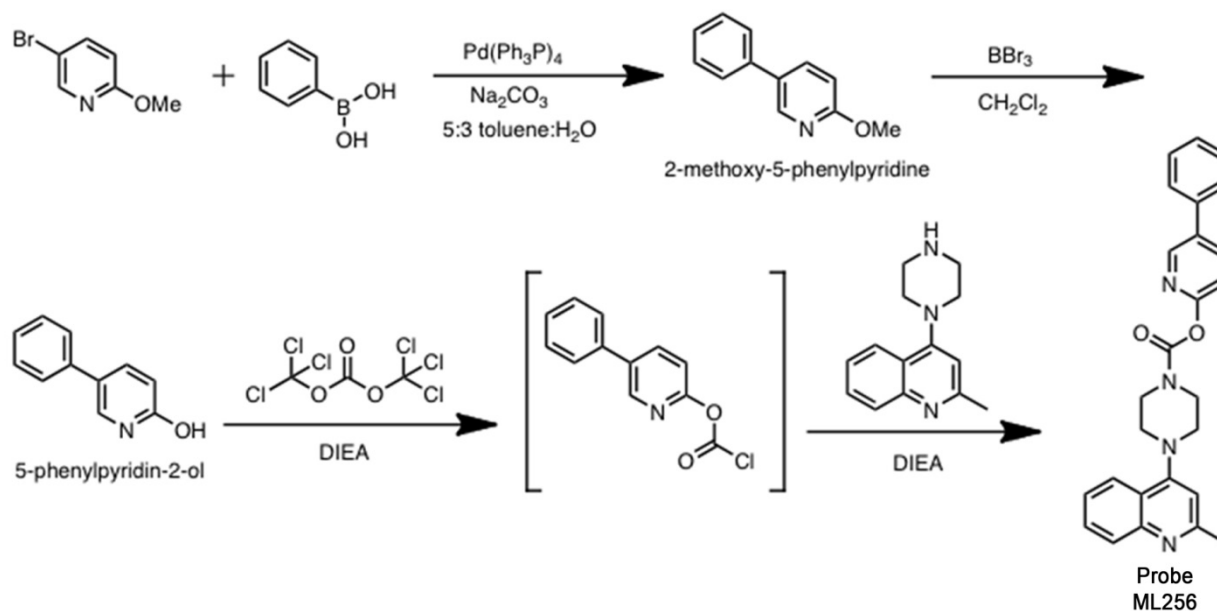
CID 53364507
SID 125269079
ML256

The probe structure was verified by ^1H NMR (see **section 2.3**) and high resolution MS (m/z calculated for $\text{C}_{26}\text{H}_{24}\text{N}_4\text{O}_2$ $[\text{M}+\text{H}]^+$: 425.1972, found 425.1974). Purity was assessed to be 96% by NMR. Solubility (room temperature) was determined to be 16.3 μ M in PBS, 7.5 μ M in DMEM

medium, and >100 μM in DMEM medium containing 10% fetal calf serum. Stability in PBS was determined by LC-MS to be >48 hours.

Table 2.2-1. Compounds submitted to the SMR collection.				
Designation	CID	SID	SRID	MLS
Probe	53364507	125269079	SR-02000001715-1	MLS003874819
Analog 1	46829224	99205832	SR-02000000421-1	MLS003874820
Analog 2	53364494	125269060	SR-02000001696-1	MLS003874821
Analog 3	53364529	125269074	SR-02000001710-1	MLS003874822
Analog 4	53364548	125269075	SR-02000001711-1	MLS003874823
Analog 5	53364487	125269077	SR-02000001713-1	MLS003874824

2.3 Probe Preparation



2-methoxy-5-phenylpyridine: A mixture of 5-bromo-2-methoxypyridine (5.641 g, 30 mmol, 1.0 eq), phenylboronic acid (4.389 g, 36 mmol, 1.2 eq), Na_2CO_3 (9.539 g, 90 mmol, 3.0 eq) and $\text{Pd}(\text{PPh}_3)_4$ (1.74 g, 5 mmol%) in toluene/H₂O (v/v 5:3, 240 mL) was heated to 90°C under N_2 overnight. The product was extracted with EtOAc (3 x 300 mL) and purified by silica gel column chromatography (1-10% ethyl acetate/hexanes) to afford 2-methoxy-5-phenylpyridine (5.0571g, 27 mmol, 90%).

5-phenylpyridin-2-ol: To a solution of a 2-methoxy-5-phenylpyridine (3.13 g, 17 mmol, 1.0 eq) in dry CH_2Cl_2 (85 mL) was slowly added BBr_3 (5 g, 20 mmol, 1.2 eq) at -20°C. Upon warming to

room temperature, the reaction mixture was stirred overnight. 1N HCl (34 mL) was added to quench the reaction at 0°C. The product was extracted with ethyl acetate (3 x 170 mL). The combined organic phases were dried over NaSO₄, filtered and concentrated under reduced pressure. The product was purified by silica gel column chromatography (1-10% methanol/CH₂Cl₂) to recover unreacted starting material and afford 5-phenylpyridin-2-ol (0.0825 g, 0.5 mmol, 3%).

5-phenylpyridin-2-yl 4-(2-methylquinolin-4-yl)piperazine-1-carboxylate (Probe ML256): To a solution of triphosgene (0.0549 g, 0.185 mmol, 0.33 eq) in CH₂Cl₂ (5.55 mL), was slowly added 5-phenylpyridin-2-ol (0.0951 g, 0.555 mmol, 1.00 eq) and DIEA (97 µL, 0.0716 g, 0.555 mmol, 1.00 eq) as a solution in THF (5.55 mL). The reaction was stirred at room temperature for 30 min to generate the intermediate chloroformate. In a separate flask containing CH₂Cl₂ (5.55 mL), 2-methyl-4-piperazinoquinoline (0.1892 g, 0.833 mmol, 1.50 eq) was mixed with DIEA (146 µL, 0.1078 g, 0.833 mmol, 1.5 eq). The mixture was stirred for 5 minutes at room temperature and then dropped into the flask containing the chloroformate. The reaction mixture was stirred at room temperature for another 30 minutes and partitioned between CH₂Cl₂ (28 mL) and saturated NH₄Cl (28 mL). The organic layer was washed one more time with saturated NH₄Cl (17 mL), and dried over MgSO₄. The solvent was removed by rotary evaporation and the product was purified by silica gel column chromatography (1:1 ethyl acetate/hexanes) to afford 5-phenylpyridin-2-yl 4-(2-methylquinolin-4-yl)piperazine-1-carboxylate (Probe ML256) (0.0903 g, 0.212 mmol, 38%). ¹H NMR (400 MHz, CDCl₃) δ 8.59 (dd, *J* = 2.5, 0.7 Hz, 1H), 8.04-7.91 (m, 3H), 7.65 (ddd, *J* = 8.3, 6.8, 1.4 Hz, 1H), 7.60-7.35 (m, 6H), 7.22 (dd, *J* = 8.4, 0.7 Hz, 1H), 6.78 (s, 1H), 4.02 (t, *J* = 4.9 Hz, 2H), 3.90 (t, *J* = 4.8 Hz, 2H), 3.2 (t, *J* = 5.2 Hz, 4H), 2.70 (s, 3H); ¹³C NMR (101 MHz, CDCl₃) δ 159.71, 157.84, 156.62, 153.10, 149.50, 146.76, 138.30, 137.19, 135.33, 129.56, 129.50, 129.32, 128.35, 127.34, 125.17, 123.20, 121.95, 116.31, 110.07, 52.20, 52.08, 45.08, 44.30, 25.87; HRMS ESI-TOF high-acc (*M* + *H*⁺) calculated for C₂₆H₂₄N₄O₂ 425.1972, found 425.1974; purity estimate by NMR: 96%.

3 Results

Probe ML256 has IC₅₀ values of 31 nM and 6 nM against the mouse and human isoforms of pPAFAH, respectively (**Section 3.2**). ML256 also exhibits high selectivity (>322-fold) vs. more than 20 brain SHs and its closest homolog, PAFAH2, as assayed by gel-based ABPP (**Sections 3.4 and 3.6**). Selectivity was also confirmed for the more distantly related PAFAH family members PAFAH1b2 and PAFAH1b3 and 40+ SH enzymes by ABPP-MudPIT (**Section 3.6**). ML256 was shown to be highly active against pPAFAH both *in situ* and *in vivo* (**Section 3.5**).

3.1 Summary of Screening Results

In the primary fluopol-ABPP pPAFAH HTS Assay (AID 463082), ~326K compounds were tested for inhibition of enzyme labeling by the SH-specific activity-based probe FP-Rh [18]. The assay was conducted in singlicate at 3.39 µM compound concentration using purified, recombinant human enzyme. A total of 4,934 compounds (1.5%) were active, passing the set threshold

(mean + 3x standard deviation) of 24.55% inhibition. A total of 2,500 compounds were selected for testing in the confirmation assay (AID 463230), in which compounds were re-tested at the same concentration in triplicate. Of the 2,341 available compounds, 1,675 (71.6%) confirmed as active (**Figure 3.1-1**).

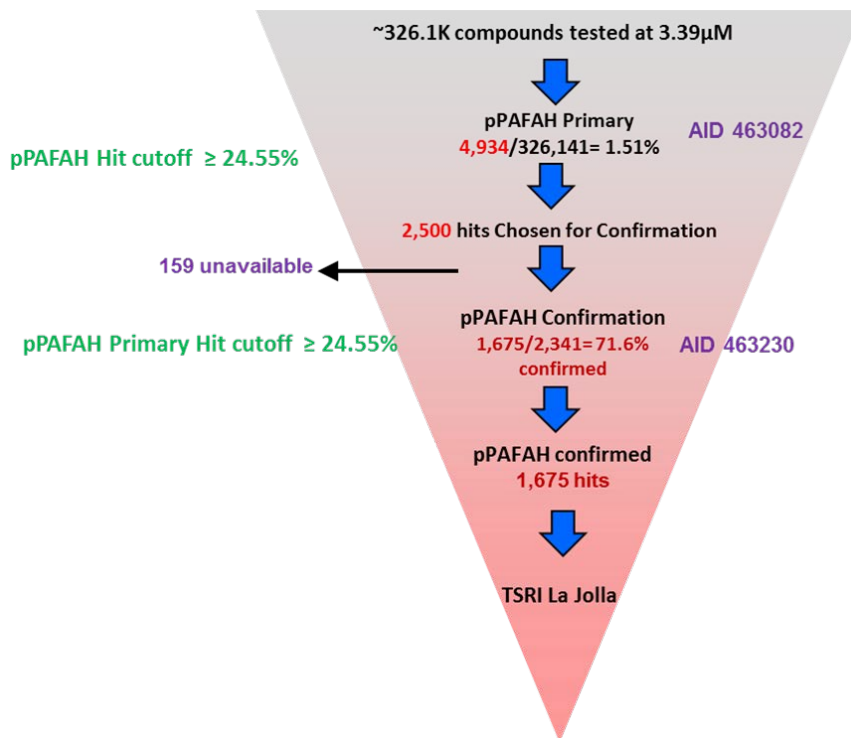


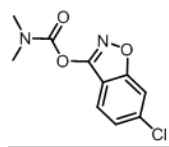
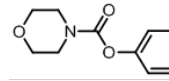
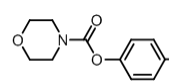
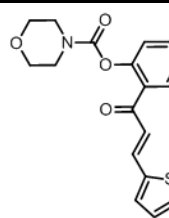
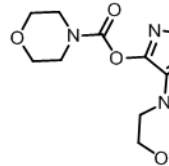
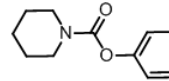
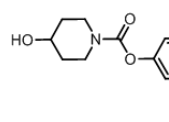
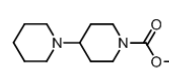
Figure 3.1-1. Flow chart describing HTS results.

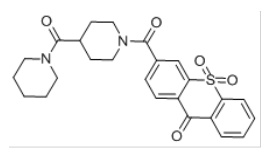
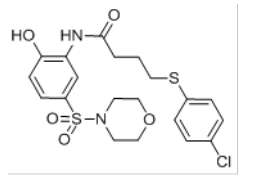
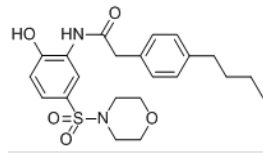
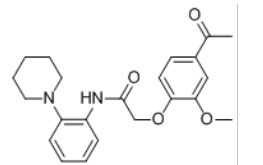
Because the fluopol-ABPP HTS assay was conducted with purified, recombinant enzyme, we selected a subset of active compounds for secondary gel-based screening to assess pPAFAH inhibition in a complex proteome. Compounds were cherry-picked from among the top HTS hits using the following criteria: in the confirmation HTS assay, a total of 407 compounds inhibited the target enzyme by at least 60%. Of those 407 compounds, 87 were removed due to reactivity with other select enzymes screened by fluopol-ABPP: GST01 (68, AID 1974), PME1 (5, AID 2130), PREPL (13, AID 2751), and PAD4 (1, AID 485272). Of the remaining 320 compounds, 92 exhibited more than 5% activity in all bioassays tested and were removed. Out of this group of 228 compounds, just over half were cherry picked for secondary screening based on lack of undesired functional groups (esters, hydrazines, oximes, etc.) and medchem potential. Because the carbamate scaffold was observed to feature prominently among the top HTS hits, an additional 25 carbamates were also selected for a total of 153 compounds.

For the gel-based competitive ABPP assay, a complex membrane proteome lysate prepared from 293T Hek cells overexpressing recombinant mouse pPAFAH was incubated with test compound (5 µM) followed by reaction with the FP-Rh activity-based probe. The reaction products were separated by SDS-PAGE and visualized in-gel using a flatbed fluorescence scanner. Test compounds that act as pPAFAH inhibitors prevent enzyme-probe interactions,

thereby decreasing the fluorescence intensity of the protein bands. As reported in AID 588474, only twelve compounds (**Table 3.1-1**) inhibited the target enzyme by $\geq 75\%$, eight of which were carbamates (See **Figure S1** and **Table S1** for gel images and full tabulated results, respectively). Most of the carbamate compounds showed good selectivity vs. PAFAH2, the closest sequence homolog of pPAFAH, in the counterscreen HTS fluopol-ABPP assay, indicating that medchem optimization should be able to deliver a selective pPAFAH inhibitor.

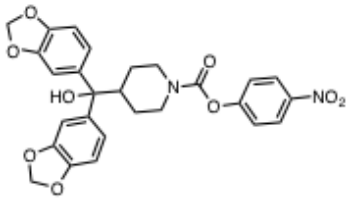
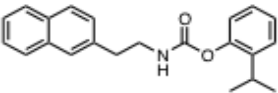
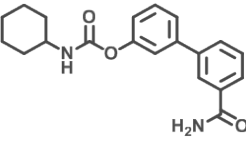
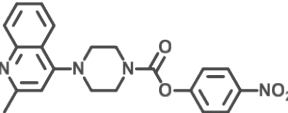
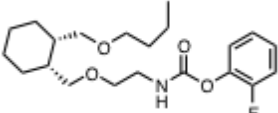
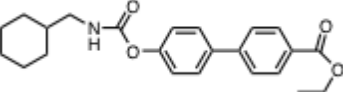
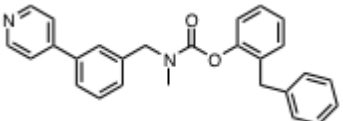
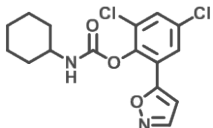
Table 3.1-1. Most promising pPAFAH inhibitor leads by gel-based competitive ABPP.

Lab Name	Structure	SID	CID	% INH pPAFAH			% INH PAFAH2	Activity all bio-assays	chemotype
				Gel-based ABPP AID 588474	HTS 1ary AID 463082	HTS 2ary AID 463230	HTS 1ary AID 492956		
J11		26727296	2726311	99%	43	52	41	9/394 (2.3%)	carbamate
P09		4257433	1378785	98%	94	98	32	15/611 (2.5%)	carbamate
B08		49677790	1582142	93%	94	97	36	6/313 (1.9%)	carbamate
A06		17413867	5734364	91%	64	61	84	17/482 (3.5%)	carbamate
I04		853294	655946	84%	85	89	31	8/626 (1.3%)	carbamate
P03		4264232	2236013	79%	44	81	0	13/605 (2.1%)	carbamate
A07		49672084	2729092	82%	94	92	26	7/321 (2.2%)	carbamate
B09		24707853	5459455	84%	34		19	3/511 (0.6%)	carbamate

G07		49645759	24747337	100%	99	93	NT	3/166 (1.8%)	other
G11		57265894	16307002	75%	91	89	79	12/215 (5.6%)	other
N08		57260648	16306230	78%	84	94	81	5/210 (2.4%)	other
I07		56315773	16231989	84%	67	68	8	5/259 (1.9%)	other

We were excited to discover promising carbamate leads for pPAFAH, as we and others have had previous success developing potent and selective serine hydrolase inhibitors based on the carbamate scaffold [28-33] (**Table 3.1-2**). The carbamate scaffold readily lends itself to diversity-oriented synthesis and medchem manipulation. Moreover, as a class, carbamates are typically active *in vivo* and have the ability to penetrate the nervous system [28, 33, 34]. We have confirmed by click chemistry-ABPP that members of this chemotype show negligible reactivity with proteins outside the SH class [35]. Within the SH class, we have previously identified carboxylesterases (CESs) as common anti-targets for carbamate inhibitors [28, 35]. In this regard, the carbamate is not unique, as the CES enzymes appear to be common targets for a variety of SH-directed inhibitors [36], likely a reflection of the role they play in xenobiotic metabolism. However, CESs are mostly restricted in their expression profile to liver [37], thus their presence as anti-targets should not affect SH characterization in most cells and tissues. For example, both the FAAH inhibitor URB597 [31] and the MAGL inhibitor JZL184 [33] (see structures **Table 3.1-2**) have proven to be highly useful chemical probes [31, 33, 38-40] despite having some CES inhibitory activity [35, 41]. Unless the target of interest is a liver enzyme, the key selectivity requirement for successful carbamate probes is to show high selectivity among all non-CES SHs. In the case of pPAFAH, we are interested in studying the effects of enzyme inhibition in the brain, so CES inhibitory activity should not be a significant concern. We have also previously addressed the issue of imperfectly selective probes by generating control “anti-probes” (see ML211 and ML226 Probe Reports), which are structurally and mechanistically similar to the optimized inhibitor but lack activity against the SH of interest, for use in parallel biological experiments to confirm functional assignments.

Table 3.1-2. Representative carbamate SH inhibitors.

SH Target	Inhibitor	Structure	-IC ₅₀ value	Reference
MAGL	JZL184		8 nM	[33]
KIAA1363	JW480		20 nM	[29]
FAAH	URB597		45 nM	[31]
pPAFAH	WWL153		290 nM*	[28]
AADAC	AS115		1 μM*	[28]
DDHD1	WWL126		< 10 μM*	[28]
ABHD2	WWL110		< 20 μM*	[28]
CES1	WWL47		< 20 μM*	[28]

* unoptimized lead inhibitor

Also included in **Table 3.1-2** is a carbamate lead inhibitor for pPAFAH, **WWL153**, which we identified from a small, in-house carbamate screening library [28]. The compound exhibited decent potency for the target enzyme, but poor selectivity, inhibiting anti-targets fatty acid amide hydrolase (FAAH) and monoacylglycerol lipase (MAGL) with only a marginal dosing window (**Table 3.4-1**). Fortuitously, the HTS carbamate hits gave us new medchem leads to further develop this scaffold (detailed in **Section 3.4**) ultimately leading us to the optimized pPAFAH probe ML256 (SID 125269079).

3.2 Dose Response Curves for Probe

IC₅₀ values for both the human (6 nM; AID 588766) and mouse (31 nM; AID 588770) isoforms of pPAFAH were obtained from gel-based competitive-ABPP data (Figure 3.2-1).

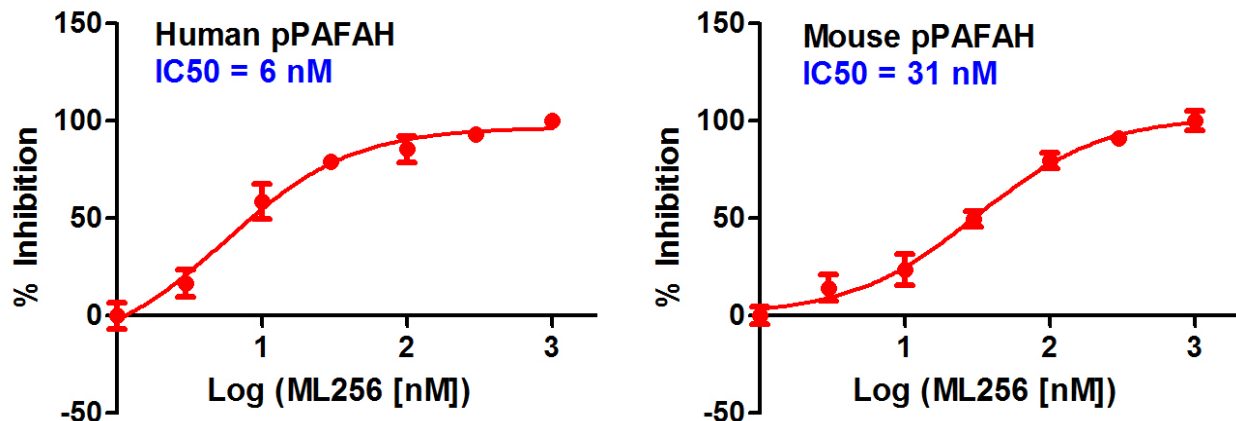
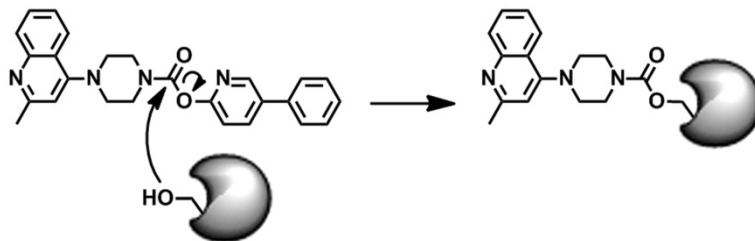


Figure 3.2-1. IC₅₀ curves for probe ML256 (SID 125269079) as determined by gel-based competitive-ABPP with FP-Rh against purified, recombinant human pPAFAH (left) and overexpressed mouse pPAFAH in a complex proteome lysate (293T Hek membrane) (right).

3.3 Scaffold/Moiety Chemical Liabilities

The probe compound was determined to covalently modify the catalytic serine (Ser273) of pPAFAH by LC-MS/MS analysis (AID 588788). The observed mass shift of the active site peptide corresponds to carbamoylation of the enzyme upon serine nucleophilic attack at the carbonyl followed by loss of the hydroxyl moiety (Figure 3.3-1), as expected of this chemotype [35].



Active Site Peptide:

K.IAVIGHS₂₇₃FGGATVIQTLSEDQR.F

Figure 3.3-1. Covalent modification of pPAFAH by ML256 (SID 125269079) as determined by LC-MS/MS analysis.

The probe compound showed no reactivity with glutathione (100 μ M), indicating that it has a tempered electrophilicity and specific structural elements that direct reactivity towards pPAFAH.

Gel-based and LC-MS/MS (MudPIT)-based ABPP selectivity profiling also confirmed high target specificity (**Section 3.6**).

We [42], and others [43-45], have found that irreversible inhibitors such as ML256 offer many advantages over reversible inhibitors as pharmacologic probes for enzyme characterization in biological systems. Perhaps most importantly, it is technically straightforward to confirm the irreversible inhibition of enzymes in living systems (including mice) using competitive ABPP and click chemistry ABPP; as such, we can define the precise quantity of inhibitor and treatment time required to selectively inactivate an enzyme of interest for biological studies. This information is extremely valuable for guiding the functional characterization of SHs. Additionally, required dosing is often lower, irreversible compounds are not as sensitive to pharmacokinetic parameters, and administration can induce long-lasting inhibition [42]. In the case of the EGFR inhibitor PD 0169414, its irreversibility and high selectivity were credited with producing prolonged inhibition of the target, alleviating concerns over short plasma half-lives and reducing the need for high peak plasma levels, thus minimizing potential nonspecific toxic effects [46].

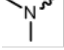
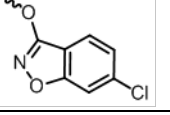
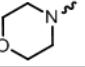
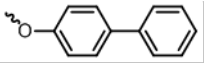
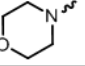
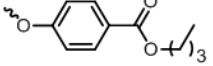
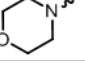
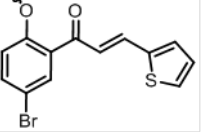
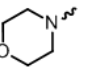
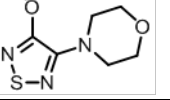
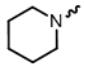
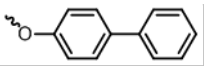
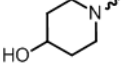
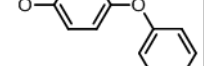
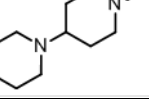
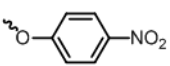
Indeed, over a third of enzymatic drug targets are irreversibly inhibited by currently marketed drugs [47]. Examples of covalent enzyme-inhibitor pairs include serine type D-Ala-D-Ala carboxypeptidase, which is covalently modified by all B-lactam antibiotics, acetylcholinesterase, whose active site serine undergoes covalent modification by pyridostigmine, prostaglandin-endoperoxide synthase, which is the target of the ubiquitously prescribed aspirin, aromatase, which is irreversibly modified by exemestane, monoamine oxidase, which is covalently modified by L-deprenyl, thymidylate synthase, which is covalently modified by floxuridine, H⁺/K⁺ ATPase, which undergoes covalent modification by omeprazole, esomeprazole, and lansoprazole, and triacylglycerol lipase, whose serine nucleophile is targeted by orlistat [47].

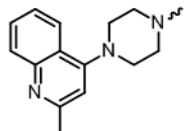
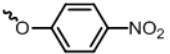
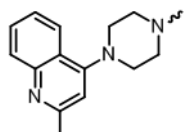
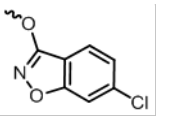
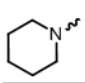
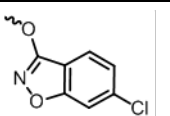
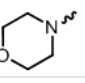
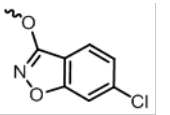
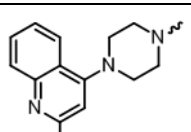
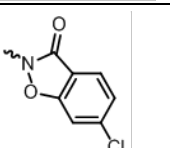
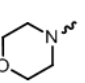
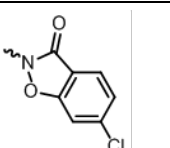
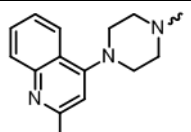
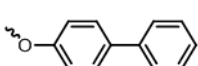
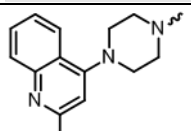
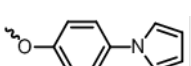
3.4 SAR Tables

The SAR **Table 3.4-1** includes 21 compounds: the top 8 carbamates identified by HTS (entries **1-8**), our in-house carbamate lead **WWL153** (entry **9**), and 12 new synthetic compounds (entries **10-21**). The analogs are variable at the left hand binding group and right hand leaving group substituents. To investigate whether or not the carbamate was the best electrophile for pPAFAH inhibition, we also generated a series of five triazole urea analogs (**Table 3.4-2**). The triazole urea reactive group is another “privileged” scaffold for SH inhibition from which we have derived several potent, selective, and *in situ*-active SH probes: ML211 as a dual inhibitor of LYPLA1&2, ML226 for ABHD11, and ML225 for the pPAFAH homolog PAFAH2 (see also ref. [48]).

All SAR compounds were subject to gel-based competitive ABPP profiling [19] to assess both potency and selectivity against several dozen FP-sensitive SHs. Because endogenous pPAFAH is difficult to visualize by gel due to low abundance and/or overlapping SHs, potency was assessed against recombinant mouse pPAFAH in the membrane proteome of 293T Hek cells engineered to overexpress the enzyme. Given our interest in exploring pPAFAH biochemistry in the brain and owing to the brain's rich diversity of anti-target SHs, selectivity was assessed using a mouse brain membrane proteome preparation. For both the potency and selectivity

analysis, compounds were tested at three concentrations: 10 μ M, 1 μ M, and 100 nM, and the gel profiling results are included in **Section 3.6** (see **Section 2.1** and AIDs 588773 and 588774 for protocol details). Proteins are listed as anti-targets for a given compound concentration if at least 50% inhibition was observed relative to the DMSO only (no compound) control. For comparison, we included the four non-carbamate HTS hits from **Table 3.1-1** in our investigation of potency and selectivity, the results (none showed pronounced inhibition of the target enzyme) are tabulated in **Table S2**.

Table 3.4-1. Target SAR Analysis					Structure		Potency and Selectivity [†]							
					Binding	Leaving	IC50 (nM) AIDs 588769 and 588770	AIDs 588773 and 588774						Fold Selectivity [§]
% INH pPAFAH			Anti-targets [‡] (mouse brain membrane)											
10 μM	1 μM	0.1 μM	10 μM	1 μM				0.1 μM						
Entry	Lab Name	SID	CID	SRID										
1	J11*	26727296	2726311	SR-01000 770684-2			234	100	92	47	FAAH, ABHD6	FAAH	FAAH	0
2	P09*	4257433	1378785	SR-01000 205082-3			469	94	78	32	FAAH	none	none	>1
3	B08*	49677790	1582142	SR-01000 254613-3			ND	90	70	5	FAAH	none	none	>1
4	A06*	17413867	5734364	SR-01000 683255-2			ND	75	56	0	FAAH	none	none	>1
5	I04*	853294	655946	SR-01000 599686-2			ND	86	28	0	FAAH	FAAH	none	0
6	P03*	4264232	2236013	SR-01000 625895-2			ND	95	33	35	FAAH, ABHD6, 30kDa	FAAH, 30kDa	none	0
7	A07*	49672084	2729092	SR-01000 645132-3			ND	92	62	0	none	none	none	>10
8	B09*	24707853	5459455	SR-01000 712294-2			ND	92	66	0	FAAH	none	none	>1

9	WWL153	99205832	46829224	SR-02000 000421-1			179	100	95	47	FAAH, MAGL	MAGL	none	0
10	JMN5	125269061	53364484	SR-02000 001697-1			ND	100	91	89	FAAH, MAGL, ABHD6, LYPLA1	FAAH, MAGL, ABHD6	FAAH, MAGL, ABHD6	0
11	JMN6	125269062	53364513	SR-02000 001698-1			ND	100	85	82	FAAH, 30kDa	FAAH	FAAH	0
12	JMN10	125269065	53364501	SR-02000 001701-1			ND	100	97	96	FAAH, ABHD6, 30kDa	FAAH	FAAH	0
13	JMN7	125269063	53364504	SR-02000 001699-1			ND	99	87	87	FAAH, MAGL, LYPLA1	FAAH, MAGL	MAGL	0
14	JMN11	125269066	53364559	SR-02000 001702-1			ND	98	98	98	FAAH, MAGL, ABHD6, 30kDa, LYPLA2, LYPLA1	FAAH, MAGL, ABHD6	FAAH	0
15	JMN4	125269060	53364494	SR-02000 001696-1			91	100	95	66	none	none	none	>109
16	JMN18	125269074	53364529	SR-02000 001710-1			57	87	80	35	none	none	none	>175

17	JMN19	125269075	53364548	SR-02000 001711-1			ND	91	82	28	none	none	none	>10
18	JMN20	125269077	53364487	SR-02000 001713-1			41	93	87	46	ABHD4	none	none	>24
19	ML256 JMN21	125269079	53364507	SR-02000 001715-1			31	100	96	67	none	none	none	>322
20	JMN22	125269081	53364545	SR-02000 001717-1			ND	56	37	2	none	none	none	>1
21	JMN23	125269083	53364525	SR-02000 001719-1			ND	95	63	2	none	none	none	>10

*MLSMR library compounds; all other (non-starred) compounds are synthetic compounds

† All IC50 data are triplicate (n=3); all % inhibition data are singlicate (n=1). Color scheme: green = IC50 < 50 nM, ≥ 50% inhibition pPAFAH, or ≥10-fold selective; grey = not determined (ND); orange = one or more anti-target(s) with >50% inhibition

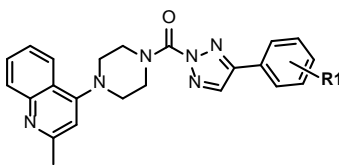
‡ Anti-targets: FAAH: fatty acid amide hydrolase; ABHD4 & 6: abhydrolase domain containing proteins 4 & 6; MAGL: monoacylglycerol lipase; LYPLA1: lysophospholipases 1; 30kDa: 30kDa protein

§ Fold Selectivity: If IC50 determined: fold selectivity = highest conc(<50% INH anti-target) / IC50 pPAFAH

If IC50 not determined: fold selectivity = highest conc(<50% INH anti-target) / lowest conc(≥50% INH pPAFAH) as reported in AIDs 588773 and 588774

If highest conc (<50% INH anti-target) < lowest conc (≥50% INH pPAFAH), then fold selectivity = 0

If lowest conc (≥50% INH pPAFAH) is not determined, then fold selectivity is not determined (ND)

Table 3.4-2. Target SAR Analysis: Triazole Ureas*					Structure	Potency and Selectivity [†]						
						% INH pPAFAH			Anti-targets [‡] (mouse brain membrane)			Fold Selectivity
Entry	Lab Name	SID	CID	SRID	 R1	10 μM	1 μM	0.1 μM	10 μM	1 μM	0.1 μM	
						22	JMN12	125269068	53364543	SR-02000001704-1	4-OCF ₃	100
23	JMN13	125269069	53364499	SR-02000001705-1	H	99	99	99	FAAH, ABHD4, MAGL, ABHD6, 32kDa, 30kDa, LYPLA2, LYPLA1	FAAH, ABHD4, ABHD6, 30kDa, LYPLA2, LYPLA1	FAAH	0
24	JMN14	125269070	53364471	SR-02000001706-1	3,4-diCl	100	98	97	FAAH, ABHD4, ABHD6, 32kDa, 30kDa, LYPLA2, LYPLA1	FAAH, ABHD4	ABHD4	0
25	JMN15	125269071	53364502	SR-02000001707-1	4-NO ₂	99	99	97	FAAH, ABHD4, MAGL, ABHD6, 32kDa, 30kDa, LYPLA2, LYPLA1	FAAH, ABHD4, MAGL, ABHD6, 32kDa, 30kDa, LYPLA2, LYPLA1	none	>1
26	JMN16	125269073	53364493	SR-02000001709-1	4-OMe	96	88	85	FAAH, ABHD4, ABHD6, 32kDa, 30kDa, LYPLA2, LYPLA1	FAAH, ABHD4, ABHD6, 32kDa, 30kDa, LYPLA2, LYPLA1	FAAH	0

*All compounds are synthetic compounds

[†] All % inhibition data are singlicate (n=1). Color scheme: green = ≥ 50% inhibition pPAFAH; orange = one or more anti-target(s) with >50% Inhibition

[‡] Anti-targets: FAAH: fatty acid amide hydrolase; ABHD 4 and 6: abhydrolase domain containing proteins 4 and 6; MAGL: monoacylglycerol lipase; LYPLA1 and 2: lysophospholipases 1 and 2; 30kDa: protein band with MW=30 kDa; 32kDa: protein band with MW=32kDa

J11/WWL153 Analogs: The development of a pPAFAH inhibitor began by combining structural elements of the top HTS hits, chiefly **J11** (SID 26727296, entry **1**) and **P09** (SID 4257433, entry **2**), with our in-house lead **WWL153** (SID 99205832, entry **9**) [28]. **WWL153** displays an IC₅₀ on the order of ~200 nM towards pPAFAH with some inhibition of FAAH and MAGL at higher (1 μM and 10 μM) concentrations, which we wanted to avoid with the final compound. We hypothesized that the 2-methyl-4-piperazinoquinoline motif was providing the majority of the potency and selectivity for our compound, especially given the predominance of piperidine-like motifs in the structures of the 12 HTS hit compounds (all but **J11**, **Table 3.1-1**). In contrast, the leaving group moieties of the HTS carbamates, while all aromatic with an emphasis on bis/bi aromatic systems (e.g., 4-hydroxybiphenyl for **P09** and **P03**, 4-phenoxyphenol for **A07**; **Table 3.4-1**, entries **2**, **6**, and **7**, respectively) evinced considerably more diversity. An especially intriguing motif was the 6-chlorobenzo[d]isoxazol-3-ol leaving group of compound **J11** (entry **1**). Out of all the HTS carbamates, **J11** displayed the best inhibition of pPAFAH in gel-based analysis (**Tables 3.1-1** and **3.4-1**). However, it also showed a strong potency towards the anti-targets FAAH and ABHD6, with persistent inhibition of the former even at low (100 nM) concentration (**Table 3.4-1**). We hypothesized that this lack in selectivity could be coming from the very simple dimethyl-amino binding group and that a more complex amine may provide better selectivity.

Based on this analysis, we synthesized a series of first generation analogs by coupling the 6-chlorobenzo[d]isoxazol-3-ol leaving group of **J11** with the 2-methyl-4-piperazinoquinoline binding group of **WWL153** to create **JMN5**, and with two prevalent amines among the HTS hits: piperidine to generate **JMN6**, and morpholine to give **JMN10** (**Table 3.4-1**, entries **10-12**). During synthesis, it was found that urea structural isomers of the 6-chlorobenzo[d]isoxazol-3-ol carbamates were formed as minor byproducts of the reaction; thus **JMN7** (isomer of **JMN5**) and **JMN11** (isomer of **JMN10**) were also synthesized and isolated for testing (**Table 3.4-1**, entries **13** and **14**). As a group, these 6-chlorobenzo[d]isoxazol-3-ol carbamates and ureas (entries **10-14**), show high potency for pPAFAH (>80% inhibition of pPAFAH at 0.1 μM; **Table 3.4-1**) but they also inhibited numerous other SHs, including FAAH, MAGL, and ABHD6, with ~equal potency. This anti-target activity suggests that the 6-chlorobenzo[d]isoxazol-3-ol leaving group overly activates the carbonyl, and that less activating leaving groups may provide better selectivity.

WWL153/Triazole Urea Analogs: Recently, our lab has investigated 1,2,3-triazole ureas as SH inhibitors (See ref. [48] and ML211, ML225 and ML226 Probe Reports). Given the potency of the urea **JMN7** (entry **13**) and the fact that we have generated selective triazole urea SH inhibitors in the past, we thought investigation of the triazole urea electrophilic scaffold for pPAFAH inhibition was merited. As such, we synthesized a series of triazole urea analogs using the 2-methyl-4-piperazinoquinoline binding group in combination with and a series of different biaromatic triazole leaving groups (**Table 3.4-2**). These compounds showed great potency towards pPAFAH (near complete inhibition observed at 0.1 μM compound concentration for all); however, they also inhibited FAAH, MAGL, and numerous other SH anti-targets with high potency as well. Due to the lack of selectivity, the triazole urea was deprioritized as scaffold for generation of a pPAFAH inhibitor.

P09/WWL153 Analogs: As mentioned before, one leaving group motif that was prevalent among the HTS carbamate hits was the 4-hydroxybiphenyl (**P09** and **P03**, **Table 3.4-1**, entries **2** and **6**). These compounds were intriguing because they not only have decent potency for inhibiting pPAFAH, but also avoid inhibiting FAAH at low concentration. The 4-hydroxybiphenyl leaving group was thus combined with the 2-methyl-4-piperazinoquinoline binding group to form **JMN4** (**Table 3.4-1**, entry **15**), which showed excellent potency for pPAFAH (IC₅₀ = 91) and the highest selectivity coefficient (>109-fold) of any synthetic compounds tested thus far.

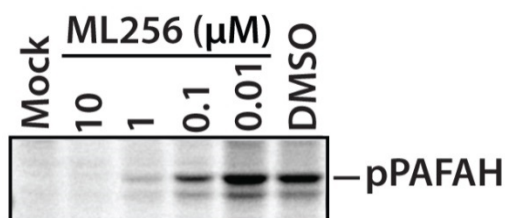
Since the 4-hydroxybiphenyl leaving group seemed important for avoiding FAAH inhibition, presumably due to its steric bulk, we proceeded to synthesize several **JMN4** analogs with biaryl or aryl-cyclo leaving groups (**JMN18-JMN23**, **Table 3.4-1**, entries **16-21**). With the exception of **JMN21** (entry **19**), all analogs displayed reduced potency (and reduced selectivity in the case of **JMN20**, entry **18**) in comparison to **JMN4**. Compound **JMN21** was ~3x more potent (IC₅₀ = 31 nM) than **JMN4** and also exhibited no anti-target effects at the highest concentration (10 μM) tested. The only difference between **JMN21** and **JMN4** is the replacement of a carbon in the phenol group with a nitrogen atom. This modification slightly activates the carbonyl, thus increasing potency. However, the biaryl system of **JMN21** prevents promiscuous binding, thus restricting this heightened reactivity to the target enzyme. This analog, **JMN21**, was designated as pPAFAH probe ML256.

Summary: As compared to our initial HTS (**J11** and **P09**) and in-house (**WWL153**) lead pPAFAH inhibitors, probe ML256 (IC₅₀ 31 nM) represents a 5-fold improvement in potency and two orders of magnitude improvement in selectivity, showing no evidence of FP-sensitive SH anti-target reactivity up to 10 μM compound concentration by gel-based ABPP.

3.5 Cellular Activity

In Situ Inhibition: Probe ML256 (SID 125269079) is active against pPAFAH *in situ* (AID 588817), inhibiting enzymatic activity by 58% at 100 nM compound concentration after 4 hours as assayed by gel-based competitive ABPP with FP-Rh (**Figure 3.5-1**). This result indicates that ML256 is free to cross cell membranes and inhibit its target in cells.

Figure 3.5-1. Inhibition of pPAFAH activity *in situ* by probe ML256 (SID 125269079). Transiently transfected 293T Hek cells overexpressing mouse pPAFAH (serum-free DMEM medium) were treated with ML256 for 4 hours, washed, harvested and the membrane fraction was isolated and subject to gel-based competitive ABPP with FP-Rh. In situ IC₅₀ is less than 0.1 μM (58% inhibition observed at 0.1 μM). Fluorescent image shown in grey scale.



In Vivo Inhibition: We also assessed the ability of probe ML256 (SID 125269079) to inhibit pPAFAH *in vivo* (AID 588823). Brain tissue was harvested from mice administered ML256 (50 mg/kg, oral gavage, 4 hour timecourse) and the membrane fraction isolated and profiled by gel-based competitive ABPP using either HT-01 (**Figure 3.5-2**, left panel) or FP-Rh (**Figure 3.5-2**, right panel). HT-01 is a triazole urea activity-based probe [27] that labels a handful of SHs in the brain, allowing enhanced visualization of pPAFAH, which is otherwise obscured by overlapping SH bands with FP-Rh profiling. In probe-treated animals, pPAFAH activity is reduced by more than 95%.

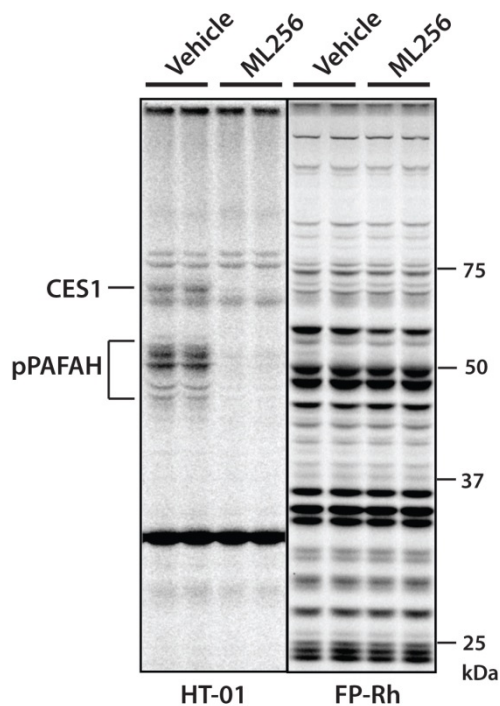


Figure 3.5-2. Inhibition of pPAFAH activity *in vivo* by probe ML256 (SID 125269079). Mice (n=2 per group) were administered ML256 (50 mg/kg via oral gavage) or vehicle only. After 4 hours, mice were sacrificed and their brain tissue removed. The membrane fraction was isolated and subject to gel-based competitive ABPP with either HT-01 (left panel) or FP-Rh (right panel). Near complete (>95%) inhibition of pPAFAH is achieved in the compound-treated samples. The only anti-target observed is CES1, an enzyme localized to the blood/liver (present due to blood contamination) whose inhibition is not expected to affect biochemical investigation of pPAFAH in the brain. Fluorescent image shown in grey scale.

There is one observed CES anti-target, CES1, which is inhibited by ML256 under these conditions (**Figure 3.5-2A**, left panel); however, CES1 is a liver enzyme [28, 37], and its presence in the membrane proteome is an artifact of blood contamination. We therefore do not believe that ML256's anti-target activity against CES1 inhibition will unduly affect biochemical profiling of pPAFAH in the brain. Regardless, we have identified other carbamate inhibitors that also inhibit CES1, but do not affect pPAFAH (e.g., **WWL47**, **Table 3.1-1** [28], or the *in vivo*-active dual KIAA1363/CES1 inhibitor **JW480** [29]), and therefore could be used as "anti-probes" for biological studies. We have previously employed a similar anti-probe strategy for the LYPLA1/2 dual inhibitor ML211, which showed inhibitory activity against anti-target ABHD11, for which we developed a selective, control "anti-probe", ML226. Other than CES1, no other anti-targets in the brain membrane proteome are observed (**Figure 3.5-2A**, right panel), a clean selectivity profile that is further substantiated by more in depth LC-MS/MS based profiling as detailed in **Section 3.6**.

Demonstrated oral bioavailability, penetration of the blood-brain barrier to deliver near complete inhibition, and a largely clean selectivity profile strongly support the utility of this probe for *in vivo*

functional and biochemical characterization of pPAFAH. It should be noted that the irreversible nature of ML256 greatly facilitates these kinds of detailed potency and selectivity analysis in living systems.

Cytotoxicity: The probe ML256 (SID 125269079) and analogs **JMN4** (SID 125269060) and **WWL153** (SID 99205832) were evaluated for cytotoxicity (AID 588768) in 293T Hek cells cultured in both serum-free and serum-supplemented medium. As shown in **Figure 3.5-3**, ML256 had significantly higher CC50 values than either analog, affording a large dosing window (50-fold) about the *in situ* IC50 value of <100 nM (**Figure 3.5-1**).

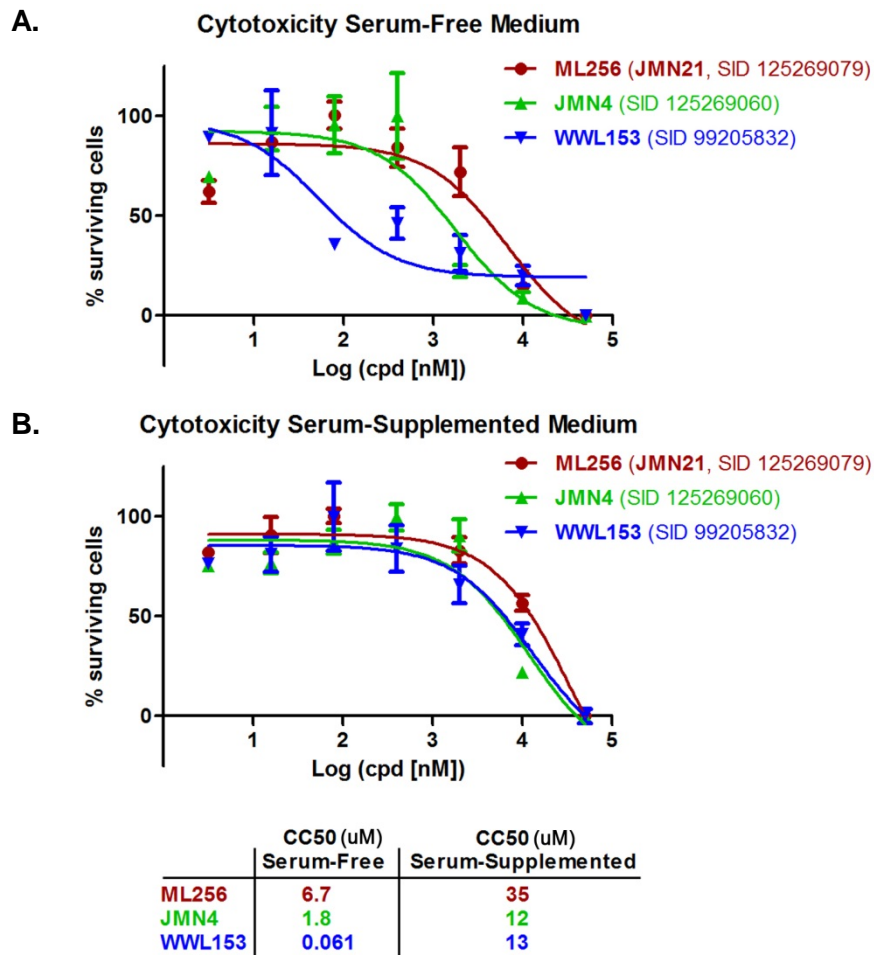


Figure 3.5-3. Cytotoxicity analysis of probe ML256 and analogs **JMN4** and **WWL153** in serum-free (**A**) and serum-supplemented (**B**) medium (AID 588768). 293T Hek cells cultured in DMEM medium with and without 10% FCS were treated with test compound and viability was assessed using the WST-1 assay (Roche) after 48 hours. ML256 showed the best cytotoxicity profile of the three compounds tested, with calculated CC50 values of >5 μ M in both assays, more than 50-fold above the *in situ* IC50 concentration (<100 nM, see **Figure 3.5-1**).

3.6 Profiling Assays

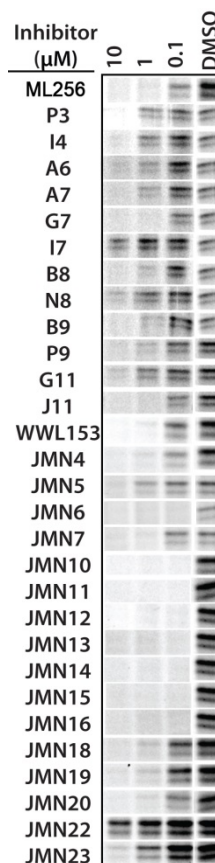
HTS Carbamates: To date, the HTS hit carbamates (**Table 3.1-1**) have all been tested in several hundred other cell-based and non-cell based bioassays deposited in PubChem, and have shown an average hit rate of 2.1%. The most reactive carbamate, **A06**, with a hit rate of 3.5%, also has a Michael acceptor functionality, which could explain its increased reactivity. This low hit rate indicates that this compound class may not be generally active. No HTS activity

data are yet available for probe ML256 or any of the synthetic analogs, nor has ML256 been submitted for commercial or non-commercial broad panel screening.

Gel-based Competitive ABPP: Probe ML256 (SID 125269079) and analogs listed in **Tables 3.4-1** and **3.4-2** have been subject to gel-based competitive ABPP screening to assess SH reactivity against more than 20 FP-sensitive SHs (including lipases, esterases, proteases, and uncharacterized hydrolases) visible by 1D SDS-PAGE separation and fluorescent detection. This medium-throughput proteome-wide screening technique was instrumental in our medchem optimization of the probe compound (**Section 3.4**), allowing rapid assessment of potency and selectivity, as visualized by disappearance of bands in compound-treated lanes relative to the DMSO-only control.

For comparative assessment of compound potency (AIDs 588773 [HTS hits] and 588774 [synthetic compounds]), **Figure 3.6-1** shows inhibition of recombinantly-expressed mouse pPAFAH in membrane proteome preparation from transiently transfected 293T Hek cells overexpressing the enzyme at three compound concentrations (10 μ M, 1 μ M, and 0.1 μ M). All data are summarized in **Tables 3.4-1**, **3.4-2**, and **S2**. As a class, the triazole ureas were the most potent compounds (showing most complete inhibition at 0.1 μ M compound concentration), but, as discussed in **Section 3.4**, they exhibited poor selectivity profiles (see **Figure 3.6-3**, lower left panel).

Figure 3.6-1. Potency of ML256 (SID 125269079) and analogs against recombinant mouse pPAFAH in a complex proteome (293T Hek cell membranes overexpressing the enzyme). For this gel-based competitive ABPP assay, proteome was incubated with test compound (10 μ M, 1 μ M, and 0.1 μ M) for 30 min, followed by reaction with FP-Rh. Reactions were separated by SDS-PAGE and visualized by in-gel fluorescent scanning. Inhibition is monitored by disappearance of the pPAFAH band relative to the DMSO control. Quantified results are summarized in **Section 3.4**. Also included in the gel figure are the four non-carbamate HTS hits (**G07**, **I07**, **N08**, and **G11**; see **Table S2** for data summary). Fluorescent image shown in grey scale.



For selectivity analysis, the competitive ABPP experiment was repeated in mouse brain membrane proteome (AIDs 588773 [HTS hits] and 588774 [synthetic compounds]). This proteome was chosen due to its relevance for future study of pPAFAH in the nervous system as well as its diversity of SHs. pPAFAH is not visible due to overlapping SH bands. Compounds were tested at the same three concentrations (10 μ M, 1 μ M, and 0.1 μ M) for determination of fold selectivity as reported in the tables in **Section 3.4**. Proteins are listed as anti-targets (Tables **Section 3.4** and **S2**) if at least 50% inhibition is observed (as quantified relative to the DMSO control) for a given compound concentration. HTS hits are shown in **Figure 3.6-2** and synthetic analogs are shown in **Figure 3.6-3**. Overall, this gel-based competitive ABPP analysis revealed that ML256 (**Figure 3.6-3**, top left panel) shows no anti-target inhibition at 10 μ M, corresponding to a large (>322-fold) selectivity window over all (>20) FP-sensitive SHs resolvable by 1D SDS-PAGE.

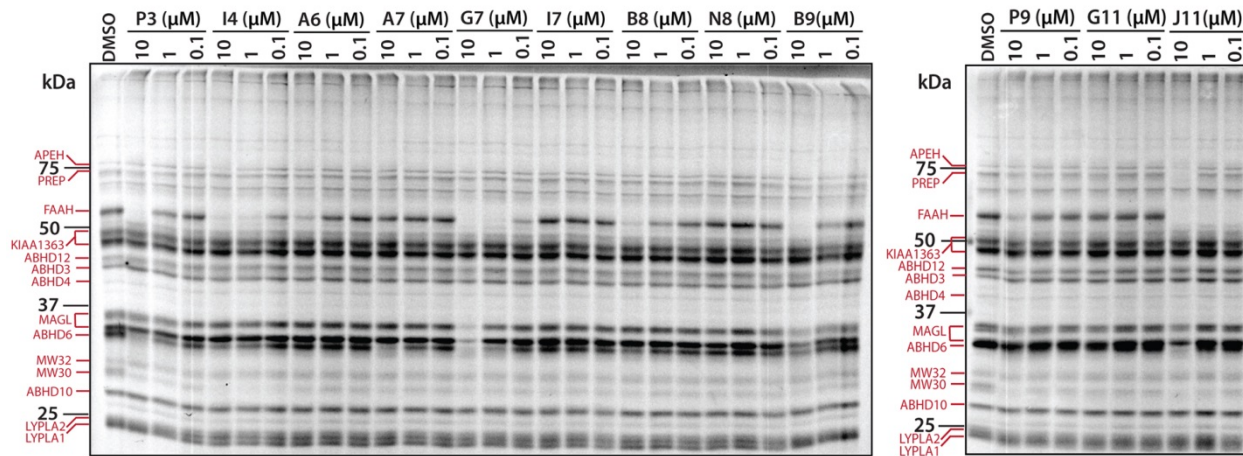


Figure 3.6-2. Selectivity of HTS hit compounds as assessed by gel-based competitive ABPP with FP-Rh in the mouse brain membrane proteome. See **Tables 3.4-1** and **S2** for summary of selectivity results. pPAFAH is not visible in these gels due to overlapping SH bands. See **Table S3** for anti-target abbreviations. Fluorescent images shown in grey scale.

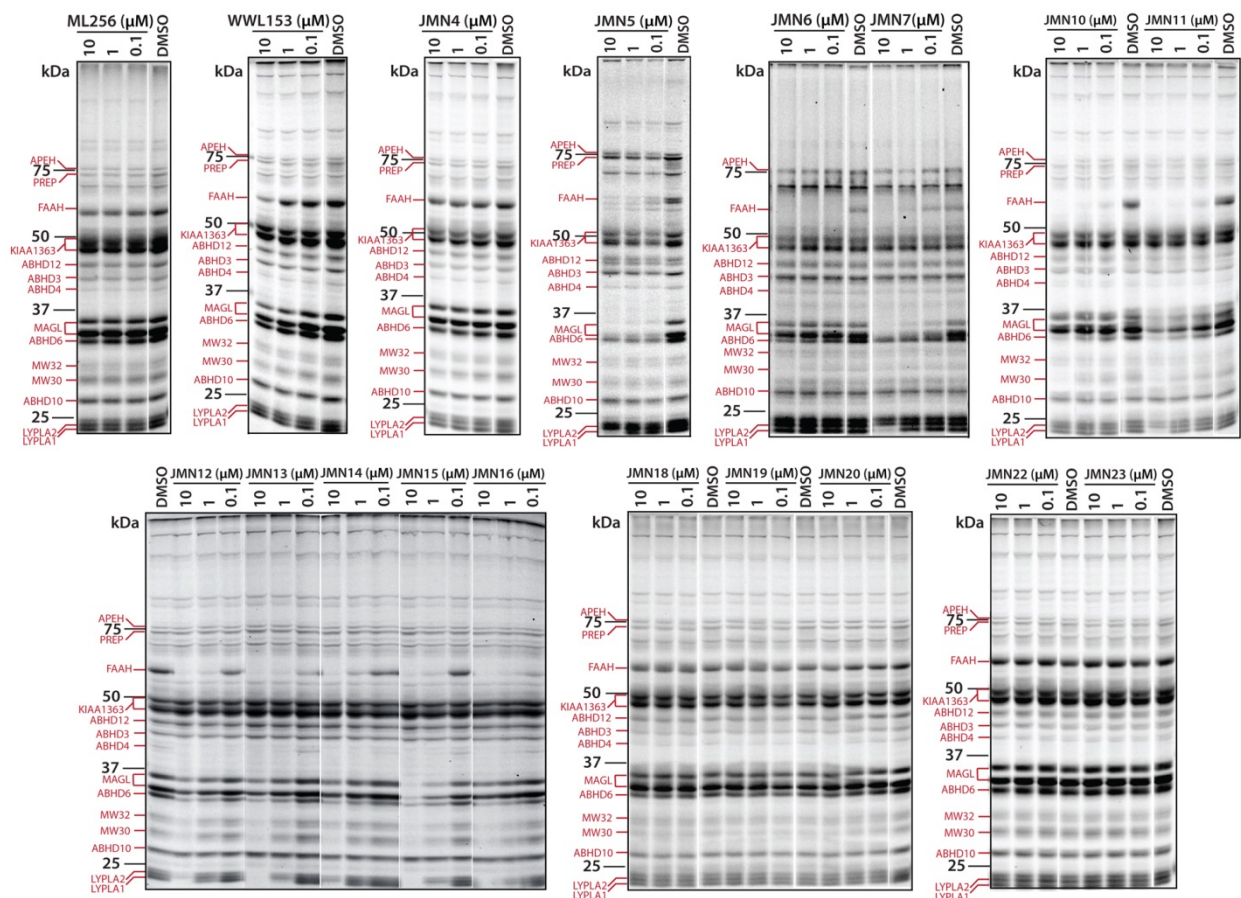
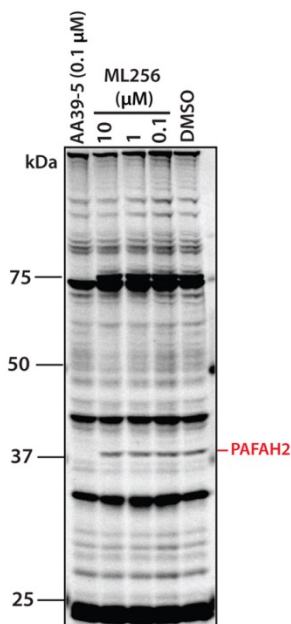


Figure 3.6-3. Selectivity of synthetic SAR compounds as assessed by gel-based competitive ABPP in the mouse brain membrane proteome. See **Tables 3.4-1** and **3.4-2** for summary of selectivity results. pPAFAH is not visible in these gels due to overlapping SH bands. See **Table S3** for anti-target abbreviations. Fluorescent images shown in grey scale.

Selectivity vs. PFAH2: Because PFAH2 is the closest sequence homolog to pPAFAH, we wanted to explicitly test the reactivity of ML256 (SID 125269079) towards this enzyme by gel-based competitive ABPP (AID 588767). For this assay, the soluble proteome of BW5147-derived murine T cells, which endogenously express PFAH2, was treated with ML256 (10 μ M, 1 μ M, and 0.1 μ M) or DMSO for 30 minutes followed by reaction with FP-Rh. Treatment with **AA39-5** (SID 103913575), a compound known to inhibit PFAH2 (see ML225 Probe Report), is shown as a control. No inhibition of PFAH2 is observed at 10 μ M ML256 concentration, giving fold selectivity of >322 for pPAFAH vs. PFAH2.

Figure 3.6-4. Selectivity of ML256 (SID 125269079) vs. PAFAH2, the closest sequence homolog of pPAFAH, as assessed by gel-based competitive ABPP with FP-Rh in the murine T-cell soluble proteome. No inhibition of anti-target PAFAH2 is observed at the highest concentration (10 μ M) tested relative to the DMSO control, giving a fold selectivity of >322. Known PAFAH2 inhibitor **AA39-5** (SID 103913575) is shown as a control. Fluorescent images shown in grey scale.



ABPP-MudPIT: To more comprehensively identify potential anti-targets, we utilized a quantitative LC-MS/MS-based platform termed competitive ABPP-MudPIT (**Figure 3.6-5A**) [49]. ABPP-MudPIT allows for robust quantitation of inhibited enzymes via comparison of the spectra counts peptides from control vs. inhibitor-treated samples. Paired samples of mouse brain membrane (AID 588785) and soluble (AID 588787) proteomes were treated with 1 μ M of ML256 or DMSO (30 minutes) followed by reaction with the affinity-tagged FP-biotin activity-based probe (5 μ M, 2 hours). Reactions were enriched with streptavidin, digested on-bead with trypsin, and analyzed by MudPIT [25, 26] using an LTQ Thermo Scientific instrument. Protein identifications and spectra counts were obtained by MS2 searching using the ProLucid (<http://fields.scripps.edu/researchtools.php>) search algorithm and filtered using DTASelect [50]. The depicted bar graphs show the relative spectra counts between inhibitor- and DMSO-treated samples for each SH identified. Enzymes susceptible to inhibition upon compound treatment would be expected to have significantly reduced spectra counts in the inhibitor-treated sample. The results (**Figure 3.6-5B** and **C**) demonstrate that ML256 exhibits significant selectivity for pPAFAH, blocking 100% of activity while not affecting any of the other 40+ SHs detected in the mouse brain proteome, with the exception of the liver enzyme CES1, consistent with gel-based profiling results (see **Section 3.5**). The other PAFAH family enzymes PAFAH1b2 and PAFAH1b3 also showed no evidence of ML256 inhibition.

Of note, we have previously determined that we could detect the SH fatty acid amide hydrolase (FAAH) at concentrations as low as 0.0005% of the total proteome (~200 copies per cell) by gel-based ABPP [18]. By comparison, we estimate that the sensitivity of a standard ABPP-MudPIT assay is at least 10-fold higher (0.00005% of the total cell proteome, or 20 copies per cell). As such, both gel-based and LC-MS/MS-based methods offer detection of low abundance SHs for a comprehensive selectivity analysis.

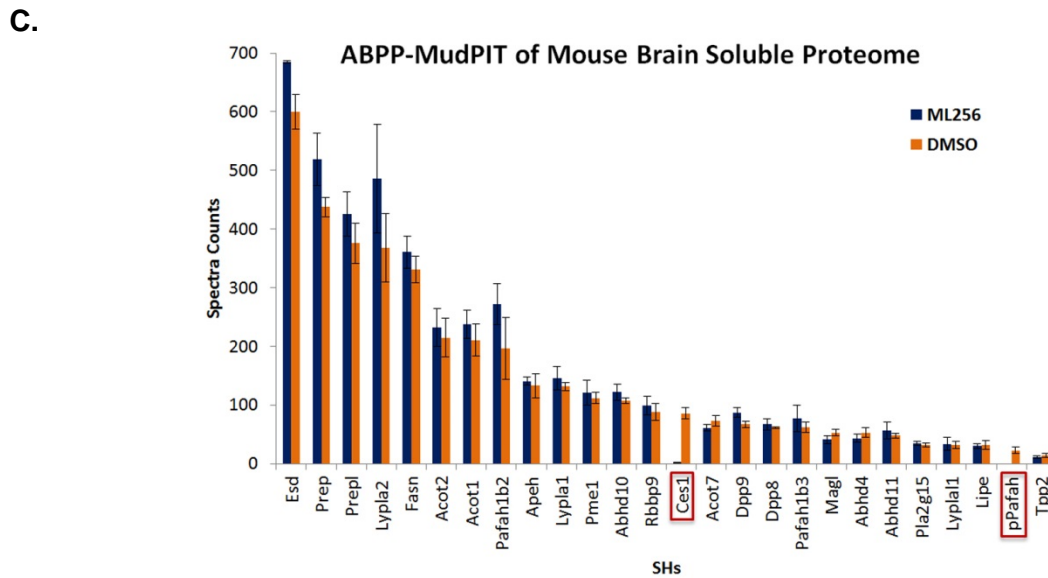
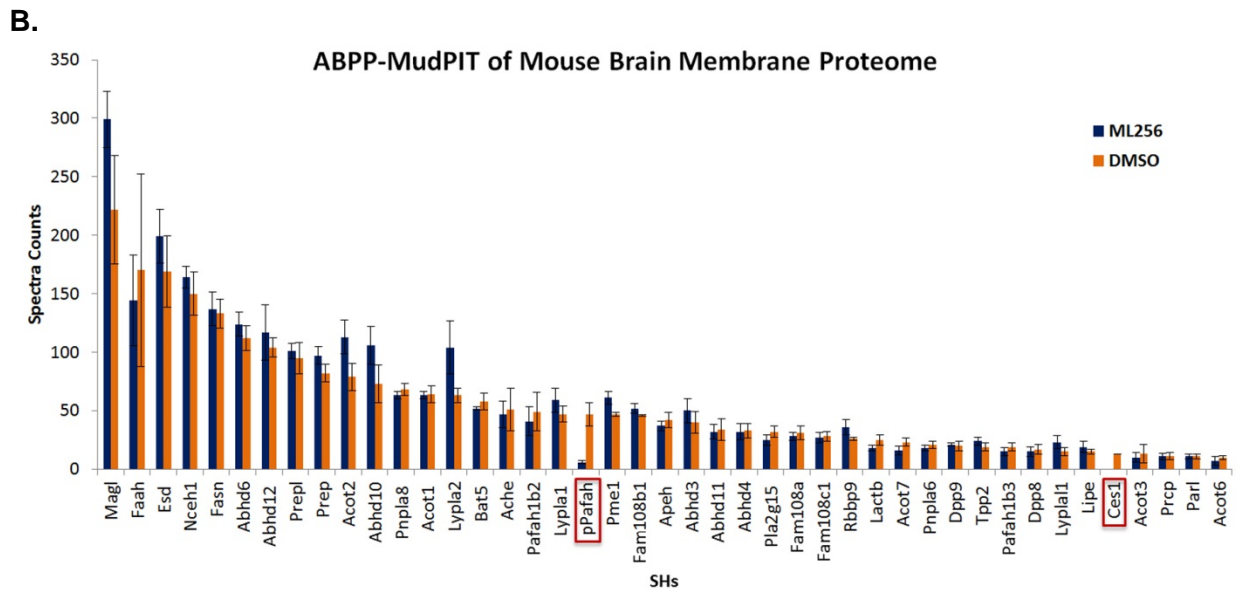
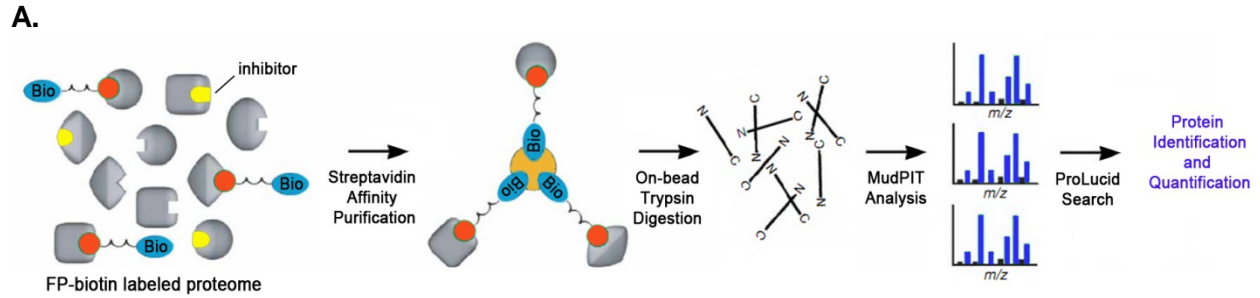


Figure 3.6-5. Potency and selectivity of ML256 assessed by ABPP-MudPIT. **A)** Overview of the ABPP-MudPIT method. **B** and **C)** Inhibition profiles of ML256 (1 μ M, 2 hour) in the mouse brain membrane (**B**) and soluble (**C**) fractions shows significant inhibition of only pPAFAH and blood artifact CES1.

4 Discussion

Probe ML256 (SID 125269079) was identified as a highly potent and selective covalent inhibitor of the target enzyme pPAFAH. The probe has an IC₅₀ of 31 nM against the mouse isoform and 6 nM against the human isoform of pPAFAH (**Section 3.2**), and very high selectivity (>322-fold) against its closest homologue PAFAH2 and all other brain-specific SH anti-targets surveyed by gel-based competitive ABPP (**Sections 3.4** and **3.6**). A more in-depth ABPP-MudPIT analysis revealed no anti-target reactivity for more than 40 SHs, with the exception of the liver enzyme CES1 (**Section 3.6**). While this anti-target activity is not expected to be problematic for investigation of the brain biology of pPAFAH, there are several CES1 inhibitors available for use as controls in biological experiments [28, 29]. ML256 is active *in situ* with an IC₅₀ <100 nM, orally bioavailable, active *in vivo*, and able to cross the blood-brain to inhibit its intended target to near completion in the brain (**Section 3.5**). Importantly, the compound shows no evidence of cytotoxicity up to 6 μM (**Section 3.5**), is stable in PBS for more than 48 hours, and easily synthesized via a three-step protocol (**Section 2.2**). Taken together, these findings suggest that it is very possible to develop potent and selective probes based on tempered electrophilic scaffolds, like the carbamate, and that ML256 will be a highly successful probe for investigation of pPAFAH biology and active-site architecture.

4.1 Comparison to existing art and how the new probe is an improvement

There were two existing pPAFAH inhibitors when we initiated our HTS campaign for inhibitor discovery: the carbamate **WWL153** (**Table 3.4-1**, entry **9**) and darapladib, a highly potent (IC₅₀ 270 pM) reversible inhibitor of pPAFAH (**Figure 4.1-1**) currently in phase III clinical trials for treatment of atherosclerosis [21, 51-55].

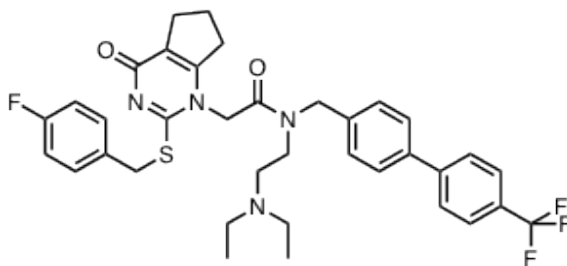


Figure 4.1-1. Structure of darapladib, a GlaxoSmithKline drug in phase III clinical trials for the treatment of atherosclerosis.

WWL153 was our best lead inhibitor for pPAFAH inhibition, and ML256 is a significant improvement in potency (>5-fold), selectivity (two orders of magnitude), and cytotoxic properties (>100-fold). We have also demonstrated that ML256 is active both *in situ* and *in vivo*. The inhibitory properties of **WWL153** in living systems have not been investigated.

Darapladib is a highly potent inhibitor of pPAFAH that operates by a reversible (non-covalent) mechanism, in contrast to the irreversible, covalent mechanism of ML256. As demonstrated in **Section 3.5**, a key advantage of ML256 is that its irreversible mechanism of action enables,

when combined with ABPP methods, direct confirmation of pPAFAH inhibition *in vivo*. Thus, persistent questions, such as the endogenous substrates of pPAFAH and the enzyme's function in the mammalian nervous system, can be assessed in mouse models with ML256. Such studies are more difficult to perform with a reversible inhibitor like darapladib, given that there are no known biomarkers that can be used to confirm the reversible inhibition of pPAFAH in living systems. As such, we view the irreversible probe ML256 as a critical addition to the chemical tools available for manipulation of pPAFAH activity for biochemical investigation.

Additionally, while darapladib is not commercially available (and very difficult to obtain from GlaxoSmithKline in sufficient quantities for comprehensive biological studies), we will make ML256 available to any investigator interested in studying pPAFAH biology. Unfortunately there is also no straightforward way to circumvent darapladib commercial unavailability through in-house synthesis. There is no detailed synthetic route published for the compound, and the synthetic overview provided in *Bioorg. Med. Chem. Lett.* [21] was not sufficiently detailed to allow, in our hands, successful resynthesis of the compound. In contrast, ML256 is easily synthesized in three steps from commercially available starting materials and a detailed protocol is included in **Section 2.3**.

Finally, one key aim of our HTS inhibitor discovery campaign was to find new scaffolds for co-crystallization studies of pPAFAH-inhibitor complexes to further define the active site and substrate specificity of pPAFAH. Attempts to crystallize pPAFAH with darapladib have been unsuccessful; however, the medchem campaign to optimize a lead carbamate inhibitor for pPAFAH has generated a diversity of potent analogs that may lend themselves to crystallographic study (in progress).

4.2 Mechanism of Action Studies

As determined from LC-MS/MS analysis (AID 588788), the probe is an activity-based inhibitor that covalently labels the active site serine nucleophile, Ser273, of pPAFAH (**section 3.3**). The observed mass shift of the active site peptide is consistent with carbamoylation of the enzyme (**Figure 3.3-1**).

4.3 Planned Future Studies

We plan to comprehensively establish parameters for *in situ* and *in vivo* use and explore the target specificity of ML256 with application of alkyne analogs via click chemistry ABPP. For biological application, we plan to use ML256 as a probe for investigation of the potential role of pPAFAH in inflammatory processes by global proteomic and metabolomic profiling of pPAFAH in *in vivo* (mouse) and *in situ* (cultured cell) models of oxidative stress to identify potential metabolic pathway involvement. We will also continue to investigate ML256 and its analogs as tools for structural studies of pPAFAH active site architecture.

5 References

1. Ames, B.N., *Dietary carcinogens and anticarcinogens. Oxygen radicals and degenerative diseases.* Science, 1983. **221**(4617): p. 1256-64.
2. Halliwell, B. and J.M. Gutteridge, *Role of free radicals and catalytic metal ions in human disease: an overview.* Methods Enzymol., 1990. **186**: p. 1-85.
3. Harman, D., *The aging process.* Proc. Natl. Acad. Sci. U. S. A., 1981. **78**(11): p. 7124-8.
4. Kono, N., et al., *Protection against oxidative stress-induced hepatic injury by intracellular type II platelet-activating factor acetylhydrolase by metabolism of oxidized phospholipids in vivo.* J. Biol. Chem., 2008. **283**(3): p. 1628-36.
5. Southorn, P.A. and G. Powis, *Free radicals in medicine. II. Involvement in human disease.* Mayo. Clin. Proc., 1988. **63**(4): p. 390-408.
6. Fruhwirth, G.O., A. Loidl, and A. Hermetter, *Oxidized phospholipids: from molecular properties to disease.* Biochim. Et Biophys. Acta, 2007. **1772**(7): p. 718-36.
7. Kinnunen, P.K., *On the principles of functional ordering in biological membranes.* Chem. Phys. Lipids, 1991. **57**(2-3): p. 375-99.
8. Uchida, K., *4-Hydroxy-2-nonenal: a product and mediator of oxidative stress.* Prog. Lipid Res., 2003. **42**(4): p. 318-43.
9. Nigam, S. and T. Schewe, *Phospholipase A(2)s and lipid peroxidation.* Biochim. Et Biophys. Acta, 2000. **1488**(1-2): p. 167-81.
10. Blank, M.L., et al., *A specific acetylhydrolase for 1-alkyl-2-acetyl-sn-glycero-3-phosphocholine (a hypotensive and platelet-activating lipid).* J. Biol. Chem., 1981. **256**(1): p. 175-8.
11. Farr, R.S., et al., *Preliminary studies of an acid-labile factor (ALF) in human sera that inactivates platelet-activating factor (PAF).* Clin. Immunol. Immunopathol., 1980. **15**(3): p. 318-330.
12. Zimmerman, G.A., et al., *The platelet-activating factor signaling system and its regulators in syndromes of inflammation and thrombosis.* Crit. Care Med., 2002. **30**(5 Suppl): p. S294-301.
13. Prescott, S.M., et al., *Platelet-activating factor and related lipid mediators.* Annu. Rev. Biochem., 2000. **69**: p. 419-45.
14. Anderson, J.L., *Lipoprotein-associated phospholipase A2: an independent predictor of coronary artery disease events in primary and secondary prevention.* Am. J. Cardiol., 2008. **101**(12A): p. 23F-33F.
15. Sudhir, K., *Clinical review: Lipoprotein-associated phospholipase A2, a novel inflammatory biomarker and independent risk predictor for cardiovascular disease.* J. Clin. Endocrinol. Metab., 2005. **90**(5): p. 3100-5.
16. Wilensky, R.L. and C.H. Macphee, *Lipoprotein-associated phospholipase A(2) and atherosclerosis.* Curr. Opin. Lipidol., 2009. **20**(5): p. 415-20.
17. Karabina, S.A. and E. Ninio, *Plasma PAF-acetylhydrolase: an unfulfilled promise?* Biochim. Et Biophys. Acta, 2006. **1761**(11): p. 1351-8.
18. Jessani, N., et al., *Enzyme activity profiles of the secreted and membrane proteome that depict cancer cell invasiveness.* Proc. Natl. Acad. Sci. U. S. A., 2002. **99**(16): p. 10335-40.
19. Leung, D., et al., *Discovering potent and selective reversible inhibitors of enzymes in complex proteomes.* Nat. Biotechnol., 2003. **21**(6): p. 687-91.
20. Bachovchin, D.A., et al., *Identification of selective inhibitors of uncharacterized enzymes by high-throughput screening with fluorescent activity-based probes.* Nat. Biotechnol., 2009. **27**(4): p. 387-94.

21. Blackie, J.A., et al., *The identification of clinical candidate SB-480848: a potent inhibitor of lipoprotein-associated phospholipase A2*. *Bioorg. Med. Chem. Lett.*, 2003. **13**(6): p. 1067-70.
22. Li, X., et al., *Characterization of dasatinib and its structural analogs as CYP3A4 mechanism-based inactivators and the proposed bioactivation pathways*. *Drug Metab. Dispos.*, 2009. **37**(6): p. 1242-50.
23. Li, X., T.M. Kamenecka, and M.D. Cameron, *Bioactivation of the epidermal growth factor receptor inhibitor gefitinib: implications for pulmonary and hepatic toxicities*. *Chem. Res. Toxicol.*, 2009. **22**(10): p. 1736-42.
24. MacCoss, M.J., C.C. Wu, and J.R. Yates, 3rd, *Probability-based validation of protein identifications using a modified SEQUEST algorithm*. *Anal. Chem.*, 2002. **74**(21): p. 5593-9.
25. Washburn, M.P., D. Wolters, and J.R. Yates, 3rd, *Large-scale analysis of the yeast proteome by multidimensional protein identification technology*. *Nat. Biotechnol.*, 2001. **19**(3): p. 242-7.
26. Wolters, D.A., M.P. Washburn, and J.R. Yates, 3rd, *An automated multidimensional protein identification technology for shotgun proteomics*. *Anal. Chem.*, 2001. **73**(23): p. 5683-90.
27. Hsu, K.L. and B.F. Cravatt, *Manuscript in preparation*. 2012.
28. Bachovchin, D.A., et al., *Superfamily-wide portrait of serine hydrolase inhibition achieved by library-versus-library screening*. *Proc. Natl. Acad. Sci. U. S. A.*, 2010. **107**(49): p. 20941-6.
29. Chang, J.W., D.K. Nomura, and B.F. Cravatt, *A potent and selective inhibitor of KIAA1363/AADACL1 that impairs prostate cancer pathogenesis*. *Chem. Biol.*, 2011. **18**(4): p. 476-84.
30. Chiang, K.P., et al., *An enzyme that regulates ether lipid signaling pathways in cancer annotated by multidimensional profiling*. *Chem. Biol.*, 2006. **13**(10): p. 1041-50.
31. Kathuria, S., et al., *Modulation of anxiety through blockade of anandamide hydrolysis*. *Nat. Med.*, 2003. **9**(1): p. 76-81.
32. Li, W., J.L. Blankman, and B.F. Cravatt, *A functional proteomic strategy to discover inhibitors for uncharacterized hydrolases*. *J. Am. Chem. Soc.*, 2007. **129**(31): p. 9594-5.
33. Long, J.Z., et al., *Selective blockade of 2-arachidonoylglycerol hydrolysis produces cannabinoid behavioral effects*. *Nat. Chem. Biol.*, 2009. **5**(1): p. 37-44.
34. Long, J.Z., et al., *Dual blockade of FAAH and MAGL identifies behavioral processes regulated by endocannabinoid crosstalk in vivo*. *Proc. Natl. Acad. Sci. U. S. A.*, 2009. **106**(48): p. 20270-5.
35. Alexander, J.P. and B.F. Cravatt, *Mechanism of carbamate inactivation of FAAH: implications for the design of covalent inhibitors and in vivo functional probes for enzymes*. *Chem. Biol.*, 2005. **12**(11): p. 1179-87.
36. Zhang, D., et al., *Fatty acid amide hydrolase inhibitors display broad selectivity and inhibit multiple carboxylesterases as off-targets*. *Neuropharmacology*, 2007. **52**(4): p. 1095-105.
37. Williams, E.T., et al., *Genomic analysis of the carboxylesterases: identification and classification of novel forms*. *Mol. Phylogenet. Evol.*, 2010. **57**(1): p. 23-34.
38. Roche, M., et al., *Augmentation of endogenous cannabinoid tone modulates lipopolysaccharide-induced alterations in circulating cytokine levels in rats*. *Immunology*, 2008. **125**(2): p. 263-71.
39. Nomura, D.K., et al., *Monoacylglycerol lipase regulates a fatty acid network that promotes cancer pathogenesis*. *Cell*, 2010. **140**(1): p. 49-61.
40. Schlosburg, J.E., et al., *Chronic monoacylglycerol lipase blockade causes functional antagonism of the endocannabinoid system*. *Nat. Neurosci.*, 2010. **13**(9): p. 1113-9.

41. Long, J.Z., D.K. Nomura, and B.F. Cravatt, *Characterization of monoacylglycerol lipase inhibition reveals differences in central and peripheral endocannabinoid metabolism*. Chem. Biol., 2009. **16**(7): p. 744-53.
42. Johnson, D.S., E. Weerapana, and B.F. Cravatt, *Strategies for discovering and derisking covalent, irreversible enzyme inhibitors*. Future Med. Chem., 2010. **2**(6): p. 949-964.
43. Potashman, M.H. and M.E. Duggan, *Covalent modifiers: an orthogonal approach to drug design*. J. Med. Chem., 2009. **52**(5): p. 1231-46.
44. Singh, J., et al., *The resurgence of covalent drugs*. Nat. Rev. Drug Discov., 2011. **10**(4): p. 307-17.
45. Kodadek, T., *Rethinking screening*. Nat. Chem. Biol., 2010. **6**(3): p. 162-165.
46. Vincent, P.W., et al., *Anticancer efficacy of the irreversible EGFR tyrosine kinase inhibitor PD 0169414 against human tumor xenografts*. Cancer Chemother. Pharmacol., 2000. **45**(3): p. 231-8.
47. Robertson, J.G., *Mechanistic basis of enzyme-targeted drugs*. Biochemistry, 2005. **44**(15): p. 5561-71.
48. Adibekian, A., et al., *Click-generated triazole ureas as ultrapotent in vivo-active serine hydrolase inhibitors*. Nat. Chem. Biol., 2011. **7**(7): p. 469-78.
49. Jessani, N., et al., *A streamlined platform for high-content functional proteomics of primary human specimens*. Nat. Methods, 2005. **2**(9): p. 691-7.
50. Cociorva, D., L.T. D, and J.R. Yates, *Validation of tandem mass spectrometry database search results using DTASelect*. Curr. Protoc. Bioinformatics, 2007. **Chapter 13**: p. Unit 13 4.
51. Mohler, E.R., 3rd, et al., *The effect of darapladib on plasma lipoprotein-associated phospholipase A2 activity and cardiovascular biomarkers in patients with stable coronary heart disease or coronary heart disease risk equivalent: the results of a multicenter, randomized, double-blind, placebo-controlled study*. J. Am. Coll. Cardiol., 2008. **51**(17): p. 1632-41.
52. Serruys, P.W., et al., *Effects of the direct lipoprotein-associated phospholipase A(2) inhibitor darapladib on human coronary atherosclerotic plaque*. Circulation, 2008. **118**(11): p. 1172-82.
53. O'Donoghue, M.L., et al., *Study design and rationale for the Stabilization of pLaques using Darapladib-Thrombolysis in Myocardial Infarction (SOLID-TIMI 52) trial in patients after an acute coronary syndrome*. Am. Heart J., 2011. **162**(4): p. 613-619 e1.
54. Wilensky, R.L., et al., *Inhibition of lipoprotein-associated phospholipase A2 reduces complex coronary atherosclerotic plaque development*. Nat. Med., 2008. **14**(10): p. 1059-66.
55. Berger, J.S., et al., *Peripheral artery disease, biomarkers, and darapladib*. Am. Heart J., 2011. **161**(5): p. 972-8.

Supplemental Information

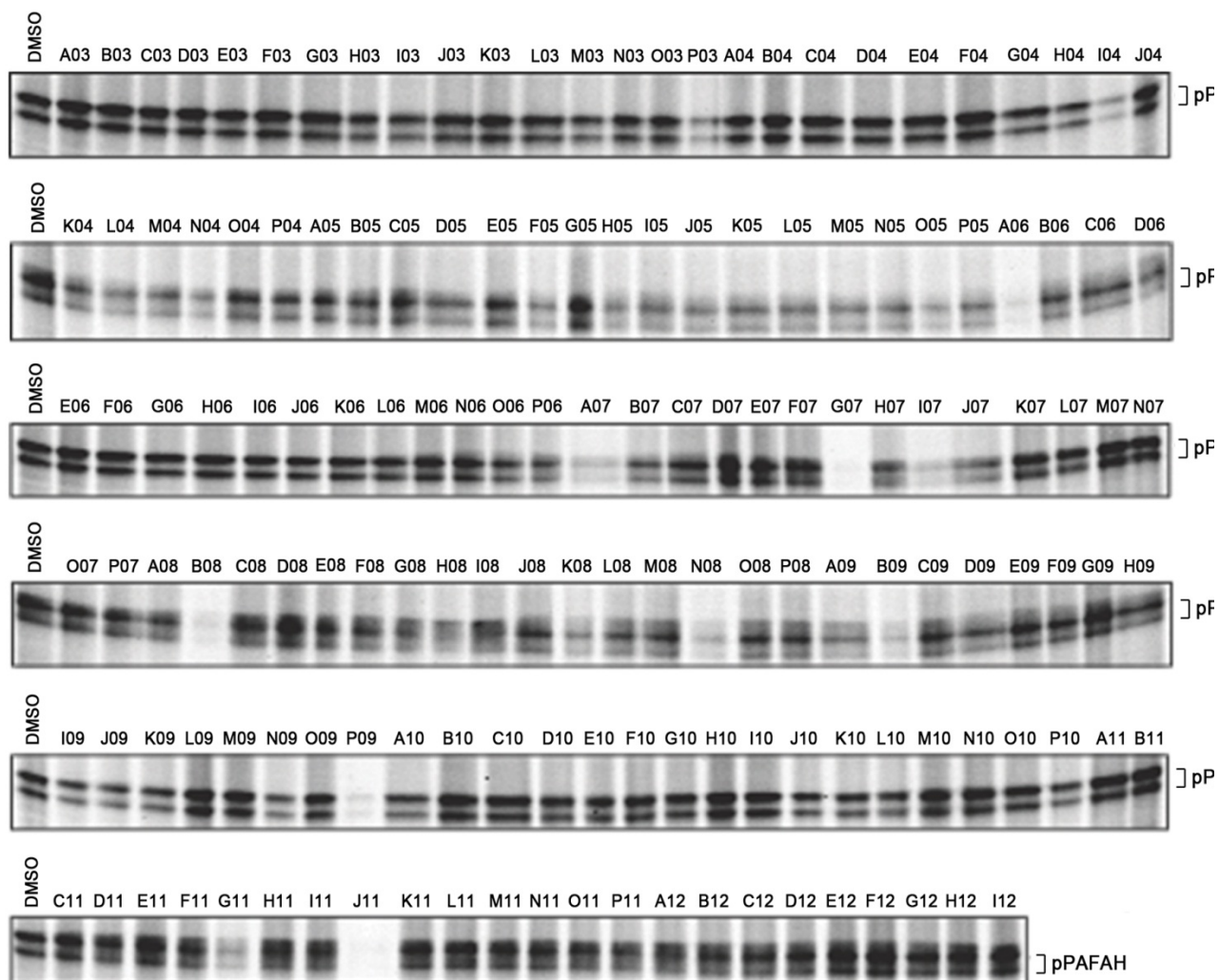


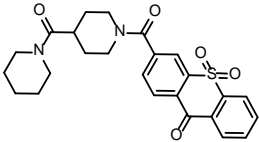
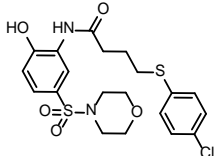
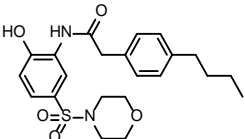
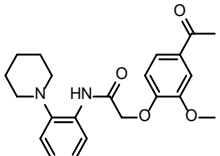
Figure S1. Gel-based competitive ABPP analysis of cherry-picked HTS hits against over-expressed pPFAH in a complex proteome (293T Hek cell lysate) at 5 μ M compound concentration (AID 588474). See **Table S1** for quantified results and compound SID/CID numbers. Fluorescent images shown in grey scale.

Table S1. Activity of cherry-picked HTS hits against pPAFAH as assessed by gel-based competitive ABPP (AID 588474)

Compound lab name	SID	CID	% Inhibition pPAFAH (5 μ M Cpd)
A03	49818553	24817488	9%
A04	49825105	4869553	36%
A05	14723122	1075762	39%
A06	17413867	5734364	91%
A07	49672084	2729092	82%
A08	49717433	4095299	31%
A09	49646777	16406874	44%
A10	49647446	4868796	34%
A11	24803039	3713423	-3%
A12	49716397	1506393	21%
B03	865529	666788	15%
B04	49647532	728803	24%
B05	49735046	4351780	30%
B06	7977938	1037259	40%
B07	24837627	4318214	44%
B08	49677790	1582142	93%
B09	24707853	5459455	84%
B10	24820189	1471280	-3%
B11	24823024	16010039	6%
B12	4244777	3239329	14%
C03	49825219	8016642	28%
C04	56463309	186136	16%
C05	17414793	5337390	23%
C06	22405959	2435938	30%
C07	49827389	24819624	10%
C08	49717475	24789974	8%
C09	4241429	3236404	13%
C10	7965604	5142655	0%
C11	85198338	3557212	19%
C12	4241939	3236852	11%
D03	4265651	893857	23%
D04	4244235	3238857	22%
D05	14735286	2901168	35%
D06	14736542	1291961	43%
D07	24789783	1092909	20%
D08	4262614	675677	5%
D09	14727785	983012	28%
D10	14746123	2251357	22%
D11	49647657	8016217	26%
D12	85269573	3642677	20%
E03	14730879	2227768	26%
E04	49717482	4299457	18%
E05	4246105	3240490	24%
E06	49719647	16031740	13%
E07	3712811	847829	17%
E08	85271190	3666144	36%
E09	4244707	3239272	10%

E10	49825244	24818849	30%
E11	57263442	7613142	7%
E12	14741589	1835517	5%
F03	845873	648231	12%
F04	49733222	2176514	5%
F05	57257880	25162008	64%
F06	24790869	5049848	10%
F07	17385991	2104350	6%
F08	49820822	4868856	31%
F09	4258391	973780	18%
F10	49717429	24789969	18%
F11	24782606	16187915	24%
F12	17385869	11839061	0%
G03	26671454	2929094	15%
G04	24818607	1483231	40%
G05	22409568	3270837	24%
G06	49717013	7573833	18%
G07	49645759	24747337	100%
G08	56323414	9314931	44%
G09	57257322	25161540	-9%
G10	49736277	24793740	21%
G11	57265894	16307002	75%
G12	14739000	2238485	8%
H03	17504315	12004490	45%
H04	7967489	651937	55%
H05	846032	648404	65%
H06	46500928	3241208	10%
H07	24791358	3271558	40%
H08	7972767	807071	55%
H09	56422452	28693	15%
H10	4251449	3245135	8%
H11	49822987	16406937	11%
H12	56324777	24983114	7%
I03	57258588	25162597	41%
I04	853294	655946	84%
I05	4265310	977306	44%
I06	49648667	16457475	23%
I07	56315773	16231989	84%
I08	49732024	6462016	22%
I09	17516379	5122563	56%
I10	49728290	1092926	3%
I11	49728289	1092856	21%
I12	4256580	1092921	7%
J03	22409711	15945323	23%
J04	3714380	2998774	38%
J05	49815912	24543718	55%
J06	56321507	24981655	28%
J07	17432567	1345082	45%
J08	56317169	24979689	16%
J09	7966421	5308219	53%
J10	56324883	24983159	42%
J11	26727296	2726311	99%
K03	85269967	2327104	21%

K04	17431795	2282503	48%
K05	14725991	1160042	43%
K06	85270454	4783698	17%
K07	49819107	2213570	12%
K08	49728592	1092738	69%
K09	14723216	1092878	38%
K10	49672846	4876778	35%
K11	17506881	2971862	8%
L03	26664791	288774	29%
L04	3716333	2084085	54%
L05	26669611	2972134	47%
L06	56324509	24982966	24%
L07	14739800	1333712	27%
L08	17508962	1150498	39%
L09	4241284	1480154	8%
L10	49829001	16406654	40%
L11	49732864	20968792	5%
M03	14733155	4048822	52%
M04	24831877	4374113	48%
M05	49823145	4869036	53%
M06	49829271	4869139	19%
M07	24823472	16195494	3%
M08	49726570	3152114	17%
M09	26729061	2795735	12%
M10	17414795	5337401	9%
M11	49665098	4869534	18%
N03	14728016	847926	41%
N04	14742766	1951620	70%
N05	49828442	16406741	53%
N06	56315412	18108581	18%
N07	14733456	3505699	18%
N08	57260648	16306230	78%
N09	14731640	1298699	57%
N10	49717138	16034280	4%
N11	56322366	24982068	20%
O03	24819918	1486626	36%
O04	7977385	749766	22%
O05	49828888	17584900	73%
O06	49829242	4967664	37%
O07	49820844	24818165	10%
O08	49645631	24747236	29%
O09	49733753	1091834	24%
O10	14739190	955142	9%
O11	49645884	16406847	21%
P03	4264232	2236013	79%
P04	49717421	4103720	41%
P05	57263037	4592650	53%
P06	17413874	2229425	46%
P07	87334149	16060009	18%
P08	14723147	1008028	30%
P09	4257433	1378785	98%
P10	14725052	1015202	46%
P11	14737509	4048820	29%

Table S2. Target SAR Analysis: non-carbamate HTS Hits					Structure	Potency and Selectivity [†]							
Entry	Lab Name	SID	CID	SRID		IC50 (nM)	AID 588773						Fold Selectivity
							% INH pPAFAH			Anti-targets [‡] (mouse brain membrane)			
							10 μM	1 μM	0.1 μM	10 μM	1 μM	0.1 μM	
	G07*	49645759	24747337	SR-01000781101-2		ND	93	88	33	FAAH, MAGL, ABHD6	FAAH	none	0
10	G11*	57265894	16307002	SR-01000863254-2		ND	88	50	18	none	none	none	>10
11	N08*	57260648	16306230	SR-01000863326-2		ND	67	15	0	none	none	none	>1
12	I07*	56315773	16231989	SR-01000843990-2		ND	34	0	0	none	none	none	ND

*MLSMR library compounds

[†] Color scheme: green = ≥ 50% inhibition pPAFAH, or ≥10-fold selective; grey = not determined (ND); orange = one or more anti-target(s) with >50% INH

[‡] Anti-targets: FAAH: fatty acid amide hydrolase; ABHD6: abhydrolase domain containing protein 6; MAGL: monoacylglycerol lipase

Table S3. Serine Hydrolase (SH) Abbreviations and Names

Abbreviation	Name	GeneID	Protein GI
pPAFAH (Pla2g7)	plasma platelet activating factor acetylhydrolase	27226	31980752
Abhd3	abhydrolase domain containing protein 3	106861	19527360
Abhd4	abhydrolase domain containing protein 4	105501	326937491
Abhd6	abhydrolase domain containing protein 6	66082	31560264
Abhd10	abhydrolase domain containing protein 10	213012	269784760
Abhd11	abhydrolase domain containing protein 11	68758	21644577
Abhd12	abhydrolase domain containing protein 12	76192	159110817
Ache	acetylcholinesterase	11423	13928664
Acot1	acyl-coenzyme A thioesterase 1	26897	6753550
Acot2	acyl-coenzyme A thioesterase 2	171210	238624114
Acot3	acyl-coenzyme A thioesterase 3	171281	19527406
Acot6	acyl-coenzyme A thioesterase 6	217700	110626167
Acot7	acyl-coenzyme A thioesterase 7	70025	225690616
Apeh	acylpeptide hydrolase	235606	19343726
Bat5	abhydrolase domain-containing protein 16A	193742	30519896
Dpp8	dipeptidyl peptidase 8	74388	31542571
Dpp9	dipeptidyl peptidase 9	224897	255003757
Ces1 (Es1)	liver carboxylesterase 1	13884	247269929
Esd	esterase D/formylglutathione hydrolase	13885	13937355
Faah	fatty acid amide hydrolase	14073	123253900
Fam108a	family with sequence similarity 108, member A	216169	21703840
Fam108b1	family with sequence similarity 108, member B1	226016	38142456
Fam108c1	family with sequence similarity 108, member C1	70178	158186616
Fasn	fatty acid synthase	14104	93102409
Kiaa1363 (Nceh1; Aadacl1)	neutral cholesterol ester hydrolase 1	320024	30520239
Lactb	lactamase, beta	80907	13507666
Lipe	hormone-sensitive lipase	16890	87239972
Lypla1	lysophospholipase 1	18777	6678760
Lypla2	lysophospholipase 2	26394	7242156
Lyplal1	lysophospholipase-like 1	226791	227496223
Magl (Mgll)	monoacylglycerol lipase	23945	261878511
Nceh1 (Aadacl1; Kiaa1363)	neutral cholesterol ester hydrolase 1	320024	30520239
Pafah1b2	platelet-activating factor acetylhydrolase IB subunit beta	18475	40254624
Pafah1b3	platelet-activating factor acetylhydrolase IB subunit gamma	18476	6679201
Parl	presenilins-associated rhomboid-like protein	381038	54261813
Pla2g15	group XV phospholipase A2 precursor	192654	19527008
Pnpla6	patatin-like phospholipase domain containing protein 6	50767	170763472
Pnpla8	patatin-like phospholipase domain containing protein 8	67452	118130807
Pme1 (Ppme1)	protein phosphatase methylesterase 1	72590	30794138
Prpc	proline carboxypeptidase	72461	33469015
Prep	prolyl endopeptidase	19072	6755152
Prepl	prolyl endopeptidase-like	213760	254939518
Rbbp9	retinoblastoma binding protein 9	26450	86439977
Tpp2	tripeptidyl peptidase 2	22019	37194903